

Stochastic Approximation with Block Coordinate Optimal Stepsizes

Tao Jiang*

Lin Xiao[†]

Abstract

We consider stochastic approximation with block-coordinate stepsizes and propose adaptive stepsize rules that aim to minimize the expected distance from the next iterate to an optimal point. These stepsize rules employ online estimates of the second moment of the search direction along each block coordinate. The popular Adam algorithm can be interpreted as a particular heuristic for such estimation. By leveraging a simple conditional estimator, we derive a new method that obtains comparable performance as Adam but requires less memory and fewer hyper-parameters. We prove that this family of methods converges almost surely to a small neighborhood of the optimal point, and the radius of the neighborhood depends on the bias and variance of the second-moment estimator. Our analysis relies on a simple aiming condition that assumes neither convexity nor smoothness, thus has broad applicability.

1 Introduction

We consider unconstrained stochastic optimization problems of the form

$$\underset{x \in \mathbf{R}^n}{\text{minimize}} \quad F(x) := \mathbf{E}_\xi[f(x, \xi)], \quad (1)$$

where $x \in \mathbf{R}^n$ is the decision variable, ξ is a random variable, and f is the loss function. In the context of statistical machine learning [e.g., 19], x represents the parameters of a prediction model, ξ represents randomly sampled data from some (unknown) probability distribution, and $f(x, \xi)$ is the error in making predictions about ξ using the model parametrized by x . We assume that F is bounded below and there exists an optimal solution x_* .

Suppose that for any pair x and ξ , we can evaluate the gradient of f with respect to x , denoted as $\nabla f(x, \xi)$. Starting with an initial point $x_0 \in \mathbf{R}^n$, the classical stochastic approximation method [42] generates a sequence $\{x_1, x_2, \dots\}$ with the update rule

$$x_{t+1} = x_t - \alpha_t \nabla f(x_t, \xi_t), \quad (2)$$

*School of Operations Research and Information Engineering (ORIE), Cornell University, Ithaca, New York, USA. Email: tj293@cornell.edu.

[†]Fundamental AI Research (FAIR) at Meta, Seattle, Washington, USA. Email: linx@meta.com.

where α_t is the stepsize (often called the *learning rate* in the machine learning literature). The convergence properties of this method are well studied in the stochastic approximation literature [e.g., 42, 54, 30]. In particular, the stepsizes α_t should be nonnegative and unsummable, i.e., $\sum_{t=0}^{\infty} \alpha_t = \infty$. Stronger guarantees such as almost sure convergence also require α_t to be square-summable, i.e., $\sum_{t=0}^{\infty} \alpha_t^2 < \infty$ [e.g., 42, 4, 7, 43].

Despite the rich literature on their convergence theory, stochastic approximation methods in practice often require heuristics and trial and error in choosing the stepsize sequence $\{\alpha_t\}$. Adaptive rules that can adjust stepsizes on the fly have been developed in both the optimization literature [e.g., 26, 35, 45, 46, 10] and by the machine learning community [e.g., 23, 50, 49, 34]. More recently, adaptive algorithms that use *coordinate-wise* stepsizes have become very popular following the seminal works of AdaGrad [14] and Adam [27], and they demonstrate significantly better performance in training large-scale deep neural networks. In this paper, we propose a family of stochastic approximation methods with block-coordinate stepsizes and present a general framework for their convergence analysis.

1.1 Stochastic approximation with block-coordinate stepsizes

We focus on stochastic approximation methods of the form

$$x_{t+1} = x_t - s_t \odot d_t, \quad (3)$$

where $d_t \in \mathbf{R}^n$ is a stochastic search direction, $s_t \in \mathbf{R}^n$ is a vector of coordinate-wise stepsizes, and \odot denotes element-wise product (Hadamard product) of two vectors. Other than using a different stepsize for each single coordinate, a block structure can be imposed where coordinates within each block share a common stepsize (see Section 1.3).

The two most common choices for the search direction are: the *stochastic gradient*, i.e., $d_t = \nabla f(x_t, \xi_t)$, and its *exponential moving average (EMA)*. Letting $g_t = \nabla f(x_t, \xi_t)$, the EMA of stochastic gradient can be expressed as

$$d_t = \beta_1 d_{t-1} + (1 - \beta_1) g_t, \quad (4)$$

where $\beta_1 \in [0, 1)$ is a smoothing factor. This is often called *stochastic momentum*.

The Adam algorithm [27] uses the stochastic momentum in (4) as its search direction and sets the coordinate-wise stepsizes as

$$s_{t,i} = \frac{\alpha_t}{\sqrt{v_{t,i}} + \epsilon}, \quad i = 1, \dots, n, \quad (5)$$

where $\alpha_t \in \mathbf{R}$ is a common stepsize *schedule* for all coordinates, $v_{t,i}$ is the EMA of $g_{t,i}^2$, and $\epsilon > 0$ is a small constant to improve numerical stability when $v_{t,i}$ becomes very close to zero. Here, computing $v_{t,i}$ requires a second smoothing factor $\beta_2 \in [0, 1]$, i.e.,

$$v_{t,i} = \beta_2 v_{t-1,i} + (1 - \beta_2) g_{t,i}^2, \quad i = 1, \dots, n. \quad (6)$$

For Adam to perform well, the second smoothing factor β_2 is often set to be larger than β_1 . For example, a pair of commonly used choices is $\beta_1 = 0.9$ and $\beta_2 = 0.99$.

Adam [27] and its variant AdamW [33] (which implements *decoupled weight decay*) have been very successful in training large-scale deep neural networks. However, theoretical understanding of their superior performance is still incomplete despite many recent efforts [e.g., 41, 5, 1, 59, 9, 58, 29]. On the other hand, there are also many works that propose new variants or alternatives to Adam and AdamW, either starting from fundamental optimization principles [e.g., 56, 17, 22, 31, 25, 37] or based on empirical algorithmic search [e.g., 6, 57]. But all have limited success. Adam and especially AdamW are still the most widely used algorithms for training large deep learning models, and their effectiveness remains a myth.

1.2 Contributions and outline

In this paper, we propose a family of *block-coordinate optimal stepsize* (BCOS) rules for stochastic approximation. BCOS gives a novel interpretation of Adam and AdamW and provides their convergence analysis as special cases of a general framework. Moreover, we derive variants of BCOS that obtain competitive performance against Adam(W) but require less memory (optimizer states) and fewer hyper-parameters. More specifically:

- In Section 2, we derive BCOS by minimizing the expected distance from the next iterate to an optimal point. While the optimal stepsizes cannot be computed exactly, we make several simplifications and approximate the second moments of the search direction with simple EMA estimators.
- In Section 3, we instantiate BCOS with specific search directions. In particular, we show that RMSProp [51] and Adam [27] can be interpreted as special cases of BCOS. With the stochastic momentum as search direction, we leverage a simple conditional estimator to derive a variant that requires fewer optimizer states and hyper-parameters than Adam. Integrating with decoupled weight decay [33] gives the BCOSW variants that enjoy comparable performance as AdamW.
- In Section 4, we present numerical experiments to compare several variants of BCOS(W) with Adam(W) on several deep learning tasks. We observe that BCOSW performs better than BCOS, and BCOSW with the conditional estimator achieves top performance with fewer optimizer states and less hyper-parameter tuning.
- In Section 5, we present the convergence analysis of BCOS(W) based on a simple aiming condition, which assumes neither convexity nor smoothness. We prove that the BCOS family of methods (including Adam and AdamW) converge almost surely to a small neighborhood of a target point, and the radius of the neighborhood depends on the bias and variance of the second-moment estimator.
- We conclude the paper in Section 6.

Generality The general form of stochastic approximation [e.g., 42, 54, 30] concerns solving a nonlinear system of equations $G(x) = 0$ where the map $G : \mathbf{R}^n \rightarrow \mathbf{R}^n$ only admits noisy evaluations in the form of $g(\cdot, \xi)$, where ξ is a random variable, under the assumption that $G(x) = \mathbf{E}_\xi[g(x, \xi)]$. In this case, stochastic approximation takes the form

$$x_{t+1} = x_t - \alpha_t g(x_t, \xi_t). \quad (7)$$

Apparently, the stochastic gradient method (2) is a special case with $g(x, \xi) = \nabla f(x, \xi)$. Although our main motivation is for solving the stochastic optimization problem (1) in the context of machine learning, the algorithms and convergence analysis developed in this paper apply to the general case of stochastic approximation with block-coordinate stepsizes.

1.3 Notations

Let $\mathcal{I}_1, \dots, \mathcal{I}_m$ be a non-overlapping partition of the index set $\{1, \dots, n\}$, each with cardinality $n_k = |\mathcal{I}_k|$. Correspondingly, we partition the vectors x_t , s_t and d_t into blocks $x_{t,k}$, $s_{t,k}$ and $d_{t,k}$ in \mathbf{R}^{n_k} for $k = 1, \dots, m$. We use a common stepsize $\gamma_{t,k} \in \mathbf{R}$ within each block, i.e., $s_{t,k} = \gamma_{t,k} \mathbf{1}_{n_k}$, where $\mathbf{1}_{n_k}$ denotes the vector of all ones of dimension n_k . As a result, the block-coordinate update in (3) can be written as

$$x_{t+1,k} = x_{t,k} - s_{t,k} \odot d_{t,k} = x_{t,k} - \gamma_{t,k} d_{t,k}, \quad k = 1, \dots, m.$$

Notice that $\gamma_{t,k}$ is always a scalar and γ_t is a vector in \mathbf{R}^m instead of \mathbf{R}^n (unless $m = n$).

Throughout this paper, $\langle \cdot, \cdot \rangle$ denotes the standard inner product in the Euclidean space \mathbf{R}^n and $\|\cdot\|$ denotes the induced Euclidean norm. For two matrices, $\langle A, B \rangle = \text{Tr}(A^T B)$.

The sign(\cdot) function is defined as $\text{sign}(\alpha) = 1$ if $\alpha > 0$, -1 if $\alpha < 0$ and 0 if $\alpha = 0$.

2 Derivation of BCOS

In this section, we first derive the ideal optimal stepsizes for block-coordinate update, which unfortunately is not computable in practice; then we make several simplifications and approximations to derive a practical algorithm.

2.1 Block-coordinate optimal stepsizes

We consider the distance of the next iterate x_{t+1} to an optimal point x_* . Specifically, in terms of the squared Euclidean distance,

$$\begin{aligned} \|x_{t+1} - x_*\|^2 &= \|x_t - s_t \odot d_t - x_*\|^2 \\ &= \|x_t - x_*\|^2 - 2\langle x_t - x_*, s_t \odot d_t \rangle + \|s_t \odot d_t\|^2. \end{aligned}$$

Exploiting the block partitions of x_t , s_t and d_t (Section 1.3) and $s_{t,k} = \gamma_{t,k} \mathbf{1}_{n_k}$, we obtain

$$\|x_{t+1} - x_*\|^2 = \|x_t - x_*\|^2 + \sum_{k=1}^m (-2\gamma_{t,k} \langle x_{t,k} - x_{*,k}, d_{t,k} \rangle + \gamma_{t,k}^2 \|d_{t,k}\|^2).$$

Taking expectation conditioned on the realization of all random variables up to x_t , i.e.,

$$\mathbf{E}_t[\cdot] := \mathbf{E}[\cdot | x_0, d_0, x_1, d_1, \dots, x_t], \quad (8)$$

we have

$$\mathbf{E}_t[\|x_{t+1} - x_*\|^2] = \|x_t - x_*\|^2 + \sum_{k=1}^m \left(-2\gamma_{t,k} \langle x_{t,k} - x_{*,k}, \mathbf{E}_t[d_{t,k}] \rangle + \gamma_{t,k}^2 \mathbf{E}_t[\|d_{t,k}\|^2] \right). \quad (9)$$

In order to minimize the expected distance from x_{t+1} to x_* , we can minimize the right-hand side of (9) over the stepsizes $\{\gamma_{t,k}\}_{k=1}^m$. This can be done separately for each block by minimizing a simple quadratic, resulting in the optimal stepsizes

$$\hat{\gamma}_{t,k} = \frac{\langle x_{t,k} - x_{*,k}, \mathbf{E}_t[d_{t,k}] \rangle}{\mathbf{E}_t[\|d_{t,k}\|^2]}, \quad k = 1, \dots, m. \quad (10)$$

Notice that these optimal stepsizes can be positive or negative, depending on the sign of the inner product in the numerator.

Plugging the optimal stepsizes into (9), we have

$$\mathbf{E}_t[\|x_{t+1} - x_*\|^2] = \|x_t - x_*\|^2 - \sum_{k=1}^m \frac{\langle x_{t,k} - x_{*,k}, \mathbf{E}_t[d_{t,k}] \rangle^2}{\mathbf{E}_t[\|d_{t,k}\|^2]}.$$

Therefore, we have a contraction of expected distance to x_* unless

$$\langle x_{t,k} - x_{*,k}, \mathbf{E}_t[d_{t,k}] \rangle = 0, \quad k = 1, \dots, m,$$

which means either $x_{t,k} = x_{*,k}$ or $\mathbf{E}_t[d_{t,k}]$ is orthogonal to $x_{t,k} - x_{*,k}$ simultaneously for all k . The latter case means that the random direction d_t contains no information that can help reduce the distance.

Apparently, the optimal stepsizes in (10) are not computable in practice, because we do not have access to x_* and cannot evaluate the expectations precisely. In the next section, we explain how to make approximations and derive a practical stepsize rule.

2.2 Simplification and approximation

We first try to avoid the direct reliance on x_* . To this end, rewrite the numerator in (10) as

$$\langle x_{t,k} - x_{*,k}, \mathbf{E}_t[d_{t,k}] \rangle = \|x_{t,k} - x_{*,k}\| \|\mathbf{E}_t[d_{t,k}]\| \cos \theta_{t,k},$$

where $\theta_{t,k}$ is the angle between the two vectors $x_{t,k} - x_{*,k}$ and $\mathbf{E}_t[d_{t,k}]$. We absorb the quantities related to x_* into a tunable parameter

$$\alpha_{t,k} = \|x_{t,k} - x_{*,k}\| \cos \theta_{t,k}, \quad (11)$$

which leads to the stepsizes

$$\tilde{\gamma}_{t,k} = \frac{\alpha_{t,k} \|\mathbf{E}_t[d_{t,k}]\|}{\mathbf{E}_t[\|d_{t,k}\|^2]}, \quad k = 1, \dots, m. \quad (12)$$

Notice that any $\alpha_{t,k}$ we choose in practice may only be a (very rough) approximation of $\|x_{t,k} - x_{*,k}\| \cos \theta_{t,k}$. In particular, while the optimal stepsizes $\hat{\gamma}_{t,k}$ can be positive or negative, it is very hard to even correctly estimate the sign of the inner product $\langle x_{t,k} - x_{*,k}, \mathbf{E}_t[d_{t,k}] \rangle$. We take the pragmatic approach of restricting $\alpha_{t,k} > 0$, effectively being *optimistic* that the expected direction $-\mathbf{E}_t[d_{t,k}]$ is always pointing towards $x_{*,k}$ (i.e., assuming $\cos \theta_{t,k} > 0$).

A further simplification is to use a common stepsize *schedule* α_t across all blocks, i.e., $\alpha_{t,k} = \alpha_t$ for all $k = 1, \dots, m$. This can be a reasonable choice for training deep neural networks, where the model parameters are initialized randomly coordinate-wise such that $\mathbf{E}[\|x_{0,k}\|]$ is constant for each coordinate k [20, 44, 13]. This brings us to

$$\tilde{\gamma}_{t,k} = \frac{\alpha_t \|\mathbf{E}_t[d_{t,k}]\|}{\mathbf{E}_t[\|d_{t,k}\|^2]}, \quad k = 1, \dots, m. \quad (13)$$

We note that with some abuse of notation, here α_t denotes a scalar, not a vector of $(\alpha_{t,1}, \dots, \alpha_{t,k})$. This simplification motivates us to link α_t to the average of $\alpha_{t,k}$ in (11) and further relate to the overall distance $\|x_t - x_*\|$. Therefore, we expect α_t to decrease as $\|x_t - x_*\|$ gradually shrinks. A simple strategy is to use a monotonic stepsize schedule on α_t , such as the popular cosine decay [32] or linear decay [8].

Next, we need to replace the conditional expectations $\mathbf{E}_t[d_{t,k}]$ and $\mathbf{E}_t[\|d_{t,k}\|^2]$ in (13) with computable approximations. We adopt the conventional approach of *exponential moving average* (EMA):

$$\begin{aligned} u_{t,k} &= \beta u_{t-1,k} + (1 - \beta) d_{t,k}, \\ v_{t,k} &= \beta v_{t-1,k} + (1 - \beta) \|d_{t,k}\|^2, \end{aligned} \quad (14)$$

where $\beta \in [0, 1)$ is the smoothing factor of EMA. Notice that $u_{t,k} \in \mathbf{R}^{n_k}$ and $v_{t,k} \in \mathbf{R}$, which have the same dimensions as $\mathbf{E}_t[d_{t,k}]$ and $\mathbf{E}_t[\|d_{t,k}\|^2]$ respectively. This leads to a set of practical stepsizes:

$$\gamma_{t,k} = \alpha_t \frac{\|u_{t,k}\|}{v_{t,k} + \epsilon}, \quad k = 1, \dots, m, \quad (15)$$

where we added a small constant $\epsilon > 0$ in the denominator to improve numerical stability (preventing overflow in case $v_{t,k}$ is too small).

2.3 BCOS with one EMA estimator

The BCOS stepsizes in (15) are easy to implement in practice, but they are computed through the ratios of two online estimators $\|u_{t,k}\|$ and $v_{t,k}$. The ratio of two random quantities may be susceptible to large fluctuations if the numerator and denominator drift in different directions (i.e., when one is much larger than its mean while the other is much smaller than its mean). To avoid this problem, we further simplify BCOS to use only one EMA estimator.

First, recall the mean-variance decomposition of the conditional second moment:

$$\mathbf{E}_t[\|d_{t,k}\|^2] = \|\mathbf{E}_t[d_{t,k}]\|^2 + \mathbf{E}_t[\|d_{t,k} - \mathbf{E}_t[d_{t,k}]\|^2] = \|\mathbf{E}_t[d_{t,k}]\|^2 + \text{Var}_t(d_{t,k}),$$

where $\text{Var}_t(d_{t,k})$ denotes the conditional variance of $d_{t,k}$. We interpret $\|\mathbf{E}_t[d_{t,k}]\|^2$ as the signal power and $\text{Var}_t(d_{t,k})$ as the noise power, and define the *signal fraction* (SiF)

$$\rho_{t,k} = \frac{\|\mathbf{E}_t[d_{t,k}]\|^2}{\mathbf{E}_t[\|d_{t,k}\|^2]} = \frac{\|\mathbf{E}_t[d_{t,k}]\|^2}{\|\mathbf{E}_t[d_{t,k}]\|^2 + \text{Var}_t(d_{t,k})}. \quad (16)$$

Apparently we have $\rho_{t,k} \in [0, 1]$, and the two boundary values of 0 and 1 correspond to the cases of zero signal and full signal (zero noise) respectively.

With the definition of SiF, we can decompose the stepsizes in (12) as

$$\tilde{\gamma}_{t,k} = \alpha_{t,k} \frac{\|\mathbf{E}_t[d_{t,k}]\|}{\mathbf{E}_t[\|d_{t,k}\|^2]} = \alpha_{t,k} \sqrt{\frac{\|\mathbf{E}_t[d_{t,k}]\|^2}{\mathbf{E}_t[\|d_{t,k}\|^2]}} \frac{1}{\sqrt{\mathbf{E}_t[\|d_{t,k}\|^2]}} = \frac{\alpha_{t,k} \sqrt{\rho_{t,k}}}{\sqrt{\mathbf{E}_t[\|d_{t,k}\|^2]}}.$$

Now we can merge $\sqrt{\rho_{t,k}} \in [0, 1]$ into the tunable parameters $\alpha_{t,k}$ and define

$$\alpha'_{t,k} := \alpha_{t,k} \sqrt{\rho_{t,k}}.$$

Then, following the same arguments as in Section 2.2, we choose to use a common stepsize schedule α'_t and obtain the practical stepsize rule

$$\gamma_{t,k} = \alpha'_t \frac{1}{\sqrt{v_{t,k}} + \epsilon}, \quad k = 1, \dots, m, \quad (17)$$

where $v_{t,k}$ is the EMA estimator of $\mathbf{E}_t[\|d_{t,k}\|^2]$ given in (14).

Another way to avoid using two estimators is to assimilate $\|\mathbf{E}_t[d_{t,k}]\|$, instead of $\sqrt{\rho_{t,k}}$, directly into the tunable parameter $\alpha'_{t,k}$ and ultimately α'_t . This would result in

$$\gamma_{t,k} = \alpha'_t \frac{1}{v_{t,k} + \epsilon}, \quad k = 1, \dots, m. \quad (18)$$

There is a major advantage of (17) over (18). Specifically, since the SiF $\rho_{t,k}$ is a dimensionless ratio, the per-iteration displacements,

$$x_{t+1,k} - x_{t,k} = \alpha'_t \frac{d_{t,k}}{\sqrt{v_{t,k}} + \epsilon},$$

are invariant of scaling of the search directions $d_{t,k}$, which makes the tuning of α'_t much easier in practice. This invariance property is also shared by Adam [27], as seen from (5) and (6). The similarity of Adam and the simplified BCOS in (17) is apparent, and we will explain their connection in detail in the next section.

Algorithm 1 BCOS-g (RMSprop)

input: $x_0, \{\alpha_t\}_{t \geq 0}, \beta \in [0, 1), \epsilon > 0$

$$v_{-1} = \nabla f(x_0, \xi_0)^2$$

for $t = 0, 1, 2, \dots$ **do**

$$g_t = \nabla f(x_t, \xi_t)$$

$$v_t = \beta v_{t-1} + (1 - \beta)g_t^2$$

$$x_{t+1} = x_t - \alpha_t \frac{g_t}{\sqrt{v_t} + \epsilon}$$

Algorithm 2 BCOS-m

input: $x_0, \{\alpha_t\}, \beta_1, \beta_2 \in [0, 1), \epsilon > 0$

$$m_{-1} = \nabla f(x_0, \xi_0)$$

$$v_{-1} = m_{-1}^2$$

for $t = 0, 1, 2, \dots$ **do**

$$g_t = \nabla f(x_t, \xi_t)$$

$$m_t = \beta_1 m_{t-1} + (1 - \beta_1)g_t$$

$$v_t = \beta_2 v_{t-1} + (1 - \beta_2)m_t^2$$

$$x_{t+1} = x_t - \alpha_t \frac{m_t}{\sqrt{v_t} + \epsilon}$$

3 Instantiations of BCOS

The derivation of BCOS in Section 2 is carried out with a general search direction d_t . In this section, we instantiate BCOS with two common choices of the search direction: the stochastic gradient and its EMA, also known as *stochastic momentum*.

To simplify presentation, we focus on the case of single-coordinate blocks, i.e., $m = n$ and $\mathcal{I}_k = \{k\}$ for $k = 1, \dots, n$. Then we can write the coordinate-wise EMA estimators $v_{t,k}$ collectively in a vector form:

$$v_t = \beta v_{t-1} + (1 - \beta)d_t^2, \quad (19)$$

where d_t^2 denotes the element-wise squared vector $d_t \odot d_t$. We also have $s_t = \gamma_t \in \mathbf{R}^n$ and

$$x_{t+1} = x_t - \gamma_t \odot d_t$$

where the vector of coordinate-wise stepsizes can be expressed as

$$\gamma_t = \alpha_t \frac{1}{\sqrt{v_t} + \epsilon} \quad (20)$$

Here $v_t + \epsilon$ means element-wise addition of ϵ , $\sqrt{v_t} + \epsilon$ denotes element-wise square root, and the fraction represents element-wise division or reciprocal. We no longer distinguish between α_t and α'_t because they are both tunable hyper-parameters.

3.1 BCOS with EMA estimator

We first present instantiations of BCOS with an EMA estimator (derived in Section 2.3).

BCOS-g Algorithm 1 is the instantiation of BCOS using $g_t = \nabla f(x_t, \xi_t)$ as the search direction, where g_t^2 denotes element-wise square and $\frac{g_t}{\sqrt{v_t} + \epsilon}$ means element-wise division. We call it BCOS-g to signify the use of gradient as search direction.

We immediately recognize that BCOS-g is exactly the RMSprop algorithm [51], which is one of the first effective algorithms for training deep neural networks. Our BCOS framework gives a novel interpretation of RMSprop and its effectiveness. In the special case with $\beta = 0$ and $\epsilon = 0$, we have $v_t = g_t^2$, and BCOS-g becomes the sign gradient method

$$x_{t+1} = x_t - \alpha_t \text{sign}(g_t), \quad (21)$$

which also received significant attention in the literature [39, 2, 47, 24].

BCOS-m Using the stochastic momentum as search direction has a long history in stochastic approximation [e.g., 18, 38, 45]. It has become the default option for modern deep learning due to its superior performance compared with using plain stochastic gradients. In Algorithm 2, we use m_t to denote the momentum, which is a standard notation in the machine learning literature. We call it BCOS-m to signify the use of momentum as the search direction. BCOS-m employs a second smoothing factor β_2 to calculate the EMA of m_t^2 . The two smoothing factors β_1 and β_2 do not need to be the same and can be chosen independently in practice. Similar to BCOS-g, the special case of BCOS-m with $\beta_2 = 0$ and $\epsilon = 0$ corresponds to the sign-momentum method

$$x_{t+1} = x_t - \alpha_t \text{sign}(m_t). \quad (22)$$

We notice that BCOS-m is very similar to Adam as given in (5) and (6). The difference is that in Adam, v_t is the EMA of g_t^2 instead of m_t^2 . From the perspective of the BCOS framework, Adam has a mismatch between the search direction m_t and the second moment estimator based on g_t^2 , which must be compensated for by using a larger smoothing factor β_2 (because m_t itself is a smoothed version of g_t). For BCOS-m, using $\beta_2 = \beta_1$ produces as good performance as Adam with the best tuned β_2 (see numerical experiments in Section 4).

In both BCOS-g and BCOS-m, we initialize $v_{-1} = g_0^2$, therefore $v_0 = g_0^2$ as well. This avoids the initial bias caused by setting $v_{-1} = 0$. An alternative way for bias correction is to initialize m_{-1} and v_{-1} as the zero vector, and then multiply m_t and v_t by $1/(1 - \beta^{t+1})$, which quickly converges to 1, as done in Adam [27]. Our numerical experiments show that these two choices do not have significant differences in practice.

3.2 BCOS with conditional estimator

Recall that the optimal stepsizes $\hat{\gamma}_{t,k}$ in (10) and their simplifications $\tilde{\gamma}_{t,k}$ in (13) are all based on *conditional* expectation. In Section 3.1, we used coordinate-wise EMA of d_t^2 to approximate the conditional expectation $\mathbf{E}_t[d_t^2]$, i.e., v_t as estimator of $\mathbf{E}_t[d_t^2]$ in BCOS-g and of $\mathbf{E}_t[m_t^2]$ in BCOS-m, respectively. In this section, we show that with m_t as the search direction, we can exploit its update form to derive effective *conditional estimators* that can avoid using EMA.

We first repeat the definition of momentum with a smoothing factor $\beta \in [0, 1)$, i.e.,

$$m_t = \beta m_{t-1} + (1 - \beta) g_t. \quad (23)$$

Algorithm 3 BCOS-c

input: $x_0, \{\alpha_t\}, \beta \in [0, 1), \epsilon > 0$

$$m_{-1} = \nabla f(x_0, \xi_0)$$

for $t = 0, 1, 2, \dots$ **do**

$$g_t = \nabla f(x_t, \xi_t)$$

$$m_t = \beta m_{t-1} + (1 - \beta)g_t$$

$$v_t = (1 - (1 - \beta)^2)m_{t-1}^2 + (1 - \beta)^2 g_t^2$$

$$x_{t+1} = x_t - \alpha_t \frac{m_t}{\sqrt{v_t} + \epsilon}$$

Algorithm 4 BCOS λ -c

input: $x_0, \{\alpha_t\}, \beta \in [0, 1), \lambda \geq 0, \epsilon > 0$

$$m_{-1} = \nabla f(x_0, \xi_0)$$

for $t = 0, 1, 2, \dots$ **do**

$$g_t = \nabla f(x_t, \xi_t)$$

$$m_t = \beta m_{t-1} + (1 - \beta)g_t$$

$$v_t = (1 - (1 - \beta)^2)m_{t-1}^2 + (1 - \beta)^2 g_t^2$$

$$x_{t+1} = (1 - \alpha_t \lambda)x_t - \alpha_t \frac{m_t}{\sqrt{v_t} + \epsilon}$$

To derive an estimator of $\mathbf{E}_t[m_t^2]$, we expand the square and take the expectation of each term:

$$\begin{aligned}
\mathbf{E}_t[m_t^2] &= \mathbf{E}_t[(\beta m_{t-1} + (1 - \beta)g_t)^2] \\
&= \beta^2 \mathbf{E}_t[m_{t-1}^2] + 2\beta(1 - \beta)\mathbf{E}_t[m_{t-1} \odot g_t] + (1 - \beta)^2 \mathbf{E}_t[g_t^2] \\
&= \beta^2 m_{t-1}^2 + 2\beta(1 - \beta)m_{t-1} \odot \mathbf{E}_t[g_t] + (1 - \beta)^2 \mathbf{E}_t[g_t^2].
\end{aligned} \tag{24}$$

where we used the fact $\mathbf{E}_t[m_{t-1}^2] = m_{t-1}^2$ and $\mathbf{E}_t[m_{t-1}] = m_{t-1}$ thanks to the definition of $\mathbf{E}_t[\cdot]$ in (8). It remains to approximate $\mathbf{E}_t[g_t]$ and $\mathbf{E}_t[g_t^2]$.

Clearly a good estimator for $\mathbf{E}_t[g_t]$ is m_t . To approximate $\mathbf{E}_t[g_t^2]$, we could use a separate EMA estimator $v'_t = \beta' v'_{t-1} + (1 - \beta')g_t^2$, but this introduces another algorithm state v'_t and a second smoothing factor β' . Meanwhile, we observe that the factor $(1 - \beta)^2$ multiplying $\mathbf{E}_t[g_t^2]$ is usually very small, especially for β close to 1. As a result, any error in approximating $\mathbf{E}_t[g_t^2]$ is attenuated by a very small factor and may not cause much difference. Therefore, for simplicity, we choose to approximate $\mathbf{E}_t[g_t^2]$ with g_t^2 itself. Combining with approximating $\mathbf{E}_t[g_t]$ with m_t , we arrive at the following *conditional* estimator for $\mathbf{E}_t[m_t^2]$:

$$v_t = \beta^2 m_{t-1}^2 + 2\beta(1 - \beta)m_{t-1} \odot m_t + (1 - \beta)^2 g_t^2. \tag{25}$$

Our numerical experiments confirmed that this indeed is a good estimator which obtains performance comparable to Adam.

While effective in practice, the estimator in (25) looks complicated and does not carry much intuition. We are motivated to derive another one that is much simpler and as effective. The key is to approximate $\mathbf{E}[g_t]$ in (24) with m_{t-1} instead of m_t , which results in

$$\begin{aligned}
v_t &= \beta^2 m_{t-1}^2 + 2\beta(1 - \beta)m_{t-1}^2 + (1 - \beta)^2 g_t^2 \\
&= (1 - (1 - \beta)^2)m_{t-1}^2 + (1 - \beta)^2 g_t^2.
\end{aligned} \tag{26}$$

This estimator is much simpler than (25). Moreover, it *resembles* the standard EMA estimator in Adam, shown in (6), with an effective smoothing factor

$$\beta' = 1 - (1 - \beta)^2,$$

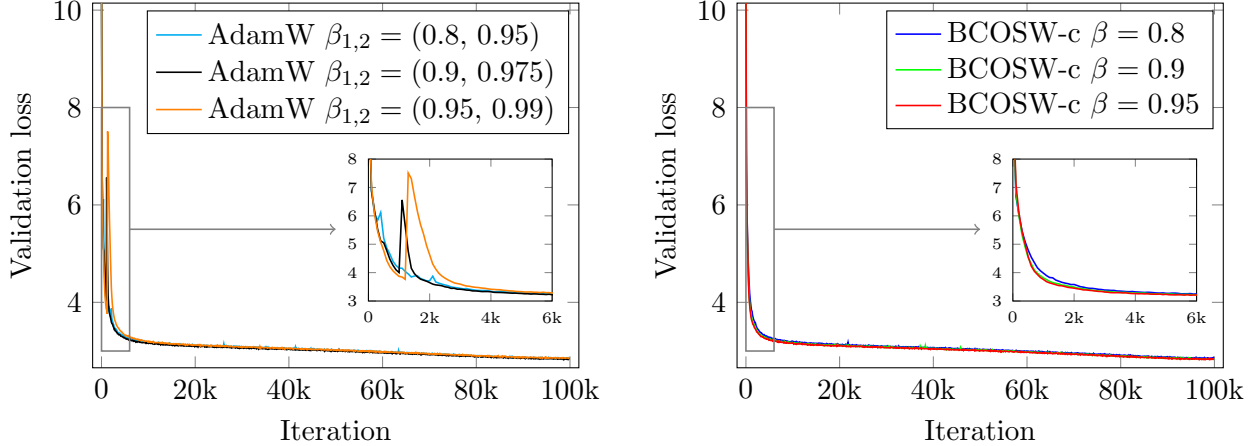


Figure 1: Comparing AdamW and BCOSW-c with different momentum parameters.

but with v_{t-1} replaced by m_{t-1}^2 . As a result, the estimator in (26) does not need to store v_{t-1} , thus requiring fewer optimizer states (less memory). This also explains that the second smoothing factor in Adam, β_2 , corresponding to β' here, should be much larger or closer to 1 than β . Specifically, $\beta = 0.9$ roughly corresponds to $\beta' = 0.99$. The estimator in (26) eliminates β_2 as a second hyper-parameter.

Finally, replacing v_t in BCOS-m with the one in (26) produces Algorithm 3. We call it BCOS-c to signify the *conditional* estimator. It has fewer optimizer states and fewer hyper-parameters to tune than BCOS-m and Adam. We note the slight abuse of notation in using the symbol v_t for both the EMA estimator in BCOS-g and -m and the conditional estimator here. In general, v_t denotes an online estimator of $\mathbf{E}_t[d_t^2]$. The corresponding choice of d_t and type of estimator should be clear from the context.

3.3 BCOS with decoupled weight decay

Weight decay is a common practice in training deep learning models to obtain better generalization performance. It can be understood as adding an L_2 regularization to the loss function, i.e., minimizing the regularized loss

$$F(x) = \mathbf{E}_\xi[f(x, \xi)] + \frac{\lambda}{2}\|x\|^2, \quad (27)$$

where $\lambda > 0$ is a regularization parameter. Effectively, the stochastic gradient at x_t becomes $\nabla f(x_t, \xi_t) + \lambda x_t$. We can apply the BCOS family of algorithms to incorporate the regularization term by simply replacing $g_t = \nabla f(x_t, \xi_t)$ with $g_t = \nabla f(x_t, \xi_t) + \lambda x_t$.

A more effective way in practice is to use *decoupled weight decay* as proposed in the AdamW algorithm [33]. Specifically, we apply weight decay separately in the BCOS update:

$$x_{t+1} = x_t - \gamma_t \odot d_t - \alpha_t \lambda x_t = (1 - \alpha_t \lambda) x_t - \gamma_t \odot d_t.$$

We call the resulting method BCOSW following the naming convention of AdamW.

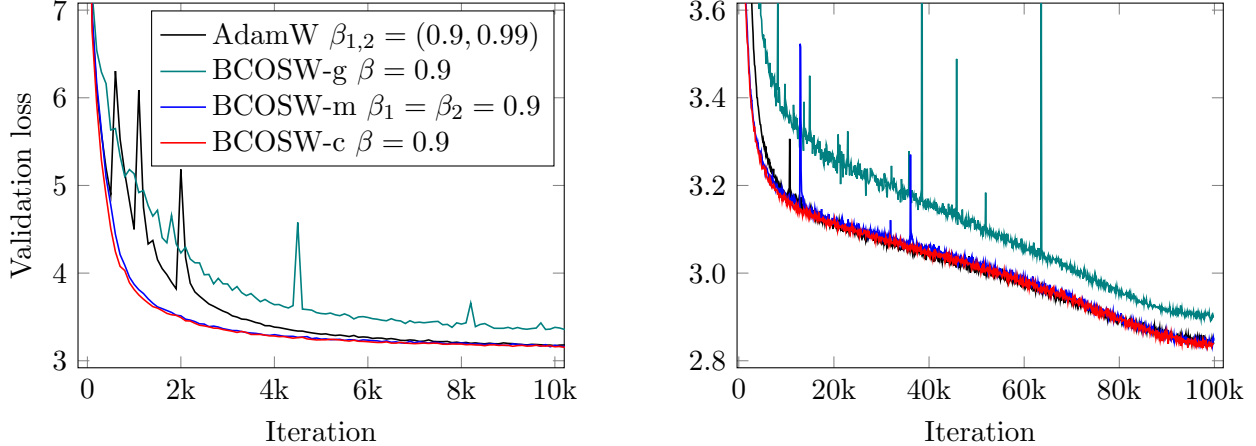


Figure 2: Comparing AdamW and three variants of BCOSW. Left: the first 10k iterations; Right: all 100k iterations.

Algorithm 4 shows BCOSW-c, which uses the conditional estimator. Other variants, namely BCOSW-g and BCOSW-m, can be obtained similarly. A PyTorch implementation of all variants of BCOS and BCOSW is given in Appendix A. The code is also available at <https://github.com/facebookresearch/bcos>.

4 Numerical experiments

In this section, we present preliminary experiments to compare BCOS with Adam, specifically their variants with decoupled weight decay. Among the BCOSW family, we focus on BCOSW-c (Algorithm 4).

Our first set of experiments is conducted on training a small GPT2 model with 124 million parameters [40] on the OpenWebText dataset [16]. We use global batch size 512 and run all experiments for 100k iterations. We use linear warmup on the stepsize schedule $\{\alpha_t\}$ to reach α_{\max} in the first 2k iterations, and then use cosine decay to toward the final stepsize $\alpha_{\min} = 0.01\alpha_{\max}$. The default hyper-parameters are chosen (based on a coarse sweep) as: peak stepsize $\alpha_{\max} = 0.002$, $\epsilon = 10^{-6}$ and weight decay $\lambda = 0.1$.

Figure 1 (left) shows the test loss of AdamW on the GPT2 task with different combinations of β_1 and β_2 . For each value of $\beta_1 \in \{0.8, 0.9, 0.95\}$, we choose the best β_2 after sweeping $\beta_2 \in \{0.8, 0.9, 0.95, 0.975, 0.99\}$. Their final losses achieved are all very close, around the value 2.82. For most (β_1, β_2) combinations, we observe some loss spikes, especially at the beginning of the training (as shown in the inset). In contrast, Figure 1 (right) shows that BCOSW-c obtains the same final loss but with very smooth loss curves.

Figure 2 compares AdamW against the three variants BCOSW-g, -m, and -c. We observe that BCOSW-g is significantly worse than the momentum-based methods. The loss curves for the momentum-based methods are all very close, but with spikes for both AdamW and BCOSW-m, while BCOSW-c has very smooth loss curves.

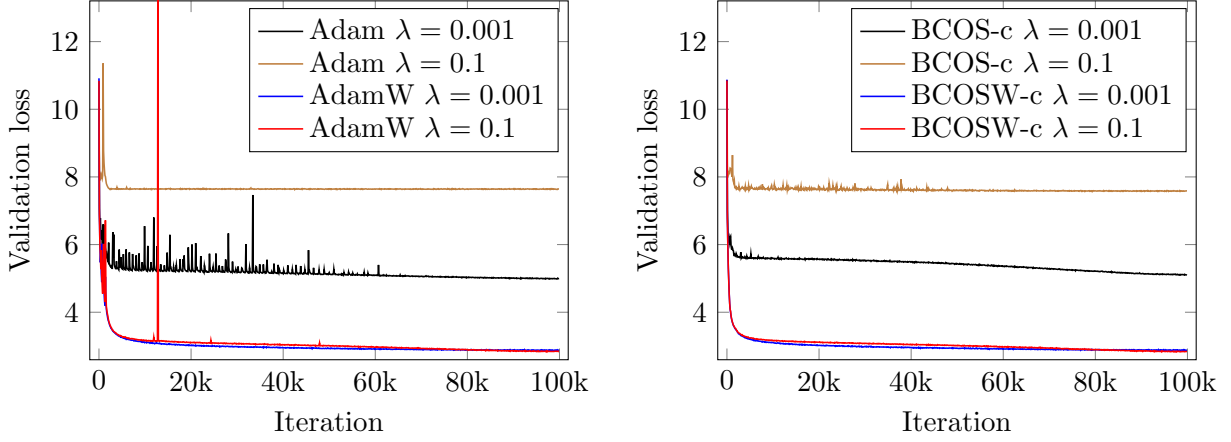


Figure 3: Left: Adam(W) with $\beta_1 = 0.9$ and $\beta_2 = 0.99$. Right: BCOS(W)-c with $\beta = 0.9$.

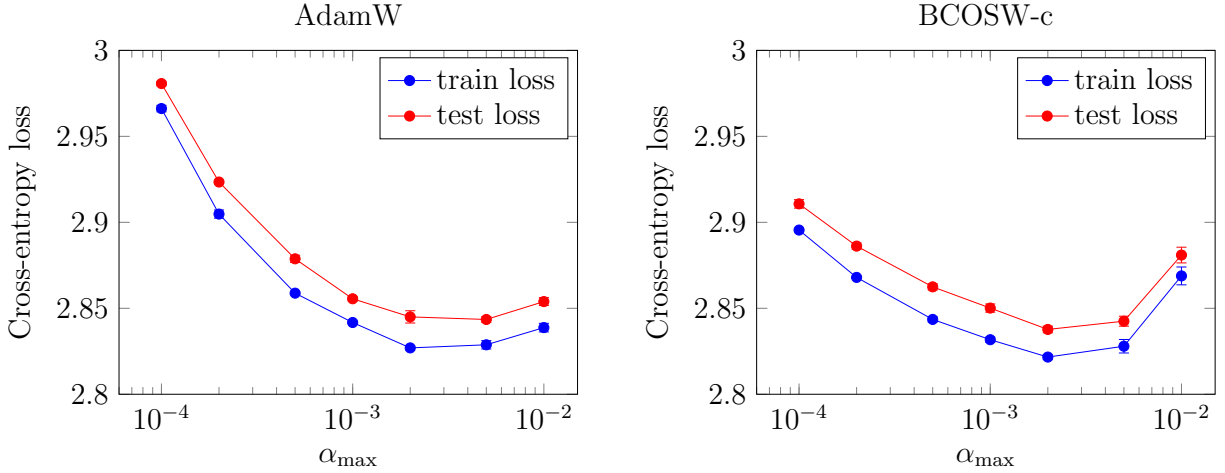


Figure 4: Train and test loss by varying max value of stepsize schedule.

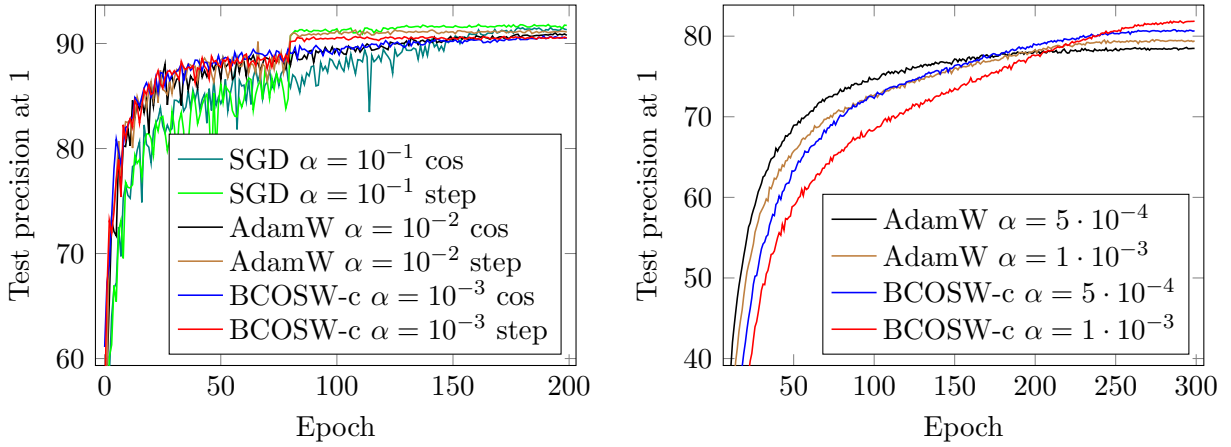


Figure 5: Left: ResNet-20 on CIFAR10. Right: Vision Transformer on ImageNet.

Figure 3 illustrates the difference between algorithms with and without decoupled weight decay. BCOS-c converges to much higher loss than BCOSW-c, and different values of λ (weight decay) make a dramatic difference for BCOS-c but cause little change to BCOSW-c. The same phenomenon happens for Adam versus AdamW, and we again observe more spikes from the loss curves of Adam(W) than BCOS(W)-c.

Figure 4 shows how the final training and validation losses (after 100k iterations) vary with α_{\max} . For each stepsize schedule, we repeat the training three times with different random seeds and plot the standard deviation as error bars, which are mostly invisible due to small variations among different runs. We observe that AdamW and BCOSW obtain the lowest losses at similar values of α_{\max} . BCOSW has slightly better performance for smaller values of α_{\max} , but becomes more sensitive for larger values of α_{\max} .

Finally, in Figure 5, we compare different algorithms for training ResNet-20 [21] on the CIFAR10 dataset [28], and also training the Vision Transformer (ViT) [52] on the ImageNet dataset [11]. For the ResNet task, we tried both cosine decay (drop by factor 100) and step decay (drop by 10 at epochs 80, 120, 150). The hyper-parameters chosen are: $\beta = 0.9$ for SGD and BCOSW-c, and $\beta_{1,2} = (0.9, 0.99)$ for AdamW. We observe that the best-performing stepsize schedules are quite different for different methods. This prompts the need to tune hyper-parameters for BCOSW for different tasks even though it shares similar tuned hyper-parameters as AdamW on the GPT2 task.

For training ViT on ImageNet, although the best tuned stepsize schedules are similar between AdamW and BCOSW, their training and test curves look quite different. Figure 5 (right) shows that the test precision curves for BCOSW-c rise slowly but reach slightly higher precision at the end.

These preliminary experiments demonstrate that BCOSW-c can obtain competitive performance compared with the state-of-the-art method AdamW, but with fewer optimizer states and fewer hyper-parameters to tune. More comprehensive empirical studies are needed to fully understand its potential in training large deep learning models.

5 Convergence analysis

In this section, we present convergence analysis for BCOS with a general search direction and decoupled weight decay (see Section 3.3). To simplify presentation, we stick with the setting of single-coordinate blocks. Specifically, we analyze the algorithm

$$x_{t+1} = (1 - \alpha_t \lambda) x_t - \gamma_t \odot d_t, \quad \text{where} \quad \gamma_t = \frac{\alpha_t}{\sqrt{v_t} + \epsilon}. \quad (28)$$

Here, stepsize γ_t takes a slightly different form from the one used throughout Section 3, where ϵ is outside the square-root in the denominator. The resulting difference between the two forms is negligible for corresponding choices of ϵ , with the one in (28) being squared (e.g., being 10^{-12} if the one in Section 3 is 10^{-6}). We choose the form in (28) for ease of presenting the analysis.

Recall that $v_t \in \mathbf{R}_+^n$ is an online estimator of $\mathbf{E}_t[d_t^2]$. Our analysis consists of two stages:

- First, we analyze the convergence behavior of the *conceptual* BCOS method

$$x_{t+1} = (1 - \alpha_t \lambda) x_t - \tilde{\gamma}_t \odot d_t, \quad \text{where} \quad \tilde{\gamma}_t = \frac{\alpha_t}{\sqrt{\mathbf{E}_t[d_t^2]}}. \quad (29)$$

It is called “conceptual” because we cannot compute $\mathbf{E}_t[d_t^2]$ exactly in practice. But its analysis is essential for understanding and analyzing the practical method. Our analysis relies on an *aiming condition*, which originates from the classical stochastic approximation literature [42, 4, 7, 48]. Under this assumption, we establish *almost sure* convergence of x_t to a target point x_* and the $\mathcal{O}(1/t)$ convergence rate of $\mathbf{E}[\|x_t - x_*\|^2]$.

- To analyze the practical BCOS method (28), we first bound the difference between the expected steps under the practical method and the conceptual method, i.e.,

$$|\mathbf{E}_t[\gamma_t \odot d_t] - \mathbf{E}_t[\tilde{\gamma}_t \odot d_t]| \leq \sigma_t |\mathbf{E}_t[\tilde{\gamma}_t \odot d_t]| + \mathcal{O}(\epsilon), \quad (30)$$

where \leq denotes coordinate-wise inequalities between two vectors and σ_t is a scalar that depends on the bias and variance of v_t as an online estimator of $\mathbf{E}_t[d_t^2]$. We prove almost sure convergence of x_t to a neighborhood of x_* , where the radius of the neighborhood is determined by the magnitude of σ_t and $\mathcal{O}(\epsilon)$.

The rest of this section is organized as follows. In Section 5.1, we introduce the aiming condition and discuss its connection with convexity. We present the convergence analysis for the conceptual BCOS method in Section 5.2 and then the analysis for the practical BCOS method in Section 5.3. Our analysis is very general and applies to the whole BCOS family of methods, including RMSprop, Adam, AdamW, and variants of spectral BCOS. To obtain specific results for each method, we only need to estimate the bias and variance of the second-moment estimator v_t , which are presented in Section 5.4.

5.1 Aiming condition

First consider the stochastic approximation method (7). A typical set of assumptions in the classical stochastic approximation literature (specifically [48]) includes:

- The random variables $\{\xi_t\}_{t \geq 0}$ are independent and $g(x, \xi)$ has bounded variance;
- The step sizes $\{\alpha_t\}_{t \geq 0}$ are nonnegative and satisfy $\sum_{t=0}^{\infty} \alpha_t = \infty$ and $\sum_{t=0}^{\infty} \alpha_t^2 < \infty$;
- Suppose $\mathbf{E}_\xi[g(x_*, \xi)] = 0$ and there exists $L, \mu > 0$ such that for all $x \in \mathbf{R}^n$,

$$L\|x - x_*\|^2 \geq \langle x - x_*, \mathbf{E}_\xi[g(x, \xi)] \rangle \geq \mu\|x - x_*\|^2. \quad (31)$$

Under these conditions, the sequence $\{x_t\}$ converges to x_* in the mean-square sense, i.e., $\lim_{t \rightarrow \infty} \mathbf{E}[\|x_t - x_*\|^2] = 0$ [48]. In particular, the last condition (31) ensures that the expected direction $\mathbf{E}_\xi[g(x, \xi)]$ always points towards the target x_* , implying that the distance from x_* can be reduced along this direction (with appropriate stepsize). For this reason, we call

it an *aiming* condition. Similar results can be established under weaker aiming conditions than (31); for example, without the upper bound on the inner product. But they are more subtle and require more sophisticated analysis [e.g., 42, 55, 3, 4, 15, 12, 54].

Following the same idea, we rewrite the conceptual BCOS method (29) as

$$x_{t+1} = x_t - \alpha_t \lambda x_t - \tilde{\gamma}_t \odot d_t = x_t - \alpha_t \left(\frac{d_t}{\sqrt{\mathbf{E}_t[d_t^2]}} + \lambda x_t \right)$$

and impose an aiming condition on the expected update direction

$$\mathbf{E}_t \left[\frac{d_t}{\sqrt{\mathbf{E}_t[d_t^2]}} + \lambda x_t \right] = \frac{\mathbf{E}_t[d_t]}{\sqrt{\mathbf{E}_t[d_t^2]}} + \lambda x_t.$$

Assumption A (Aiming condition). *There exists $x_* \in \mathbf{R}^n$ such that*

$$\left\langle x_t - x_*, \frac{\mathbf{E}_t[d_t]}{\sqrt{\mathbf{E}_t[d_t^2]}} + \lambda x_t \right\rangle \geq \lambda \|x_t - x_*\|^2 \quad (32)$$

holds for all $t \geq 0$ almost surely.

We make the following remarks regarding Assumption A.

- The condition (32) in general depends on the past trajectory $\{x_0, d_0, x_1, d_1, \dots, x_t\}$. If $\mathbf{E}_t[d_t] = \mathbf{E}[d_t|x_t]$, then we can drop the subscript t and obtain a trajectory-independent condition like (31). This is indeed the case when $d_t = g(x_t, \xi_t)$ and $\{\xi_0, \dots, \xi_t\}$ are mutually independent. We need (32) to cover more general cases, e.g., when d_t is the stochastic momentum, which clearly depends on the past trajectory.
- Instead of a generic constant μ as in (31), we have λ on the right-hand side of (32) due to the use of decoupled weight decay, interpreted as L_2 -regularization in (27).
- We do not need an upper bound on the inner product as in (31) due to the normalization effect of dividing d_t by $\sqrt{\mathbf{E}_t[d_t^2]}$ in BCOS. A similar one-sided aiming condition was used in [4] to establish almost sure convergence of the first multi-dimensional extension of the Robbins-Monro method.

Let $\rho_t \in [0, 1]^n$ be the vector of coordinate-wise SiF defined in (16). Then we have

$$\frac{\mathbf{E}_t[d_t]}{\sqrt{\mathbf{E}_t[d_t^2]}} = \sqrt{\frac{\mathbf{E}_t[d_t^2]}{\mathbf{E}_t[d_t^2]}} \text{sign}(\mathbf{E}_t[d_t]) = \sqrt{\rho_t} \odot \text{sign}(\mathbf{E}_t[d_t]).$$

Correspondingly, the aiming condition (32) can be written as

$$\langle x_t - x_*, \sqrt{\rho_t} \odot \text{sign}(\mathbf{E}_t[d_t]) + \lambda x_t \rangle \geq \lambda \|x_t - x_*\|^2. \quad (33)$$

Intuitively, the inner product in the aiming condition is predominantly determined by the coordinates that are far from optimal, in other words, the coordinates with relatively large $|x_{t,k} - x_{*,k}|$ and having a large SiF $\rho_{t,k}$ (effectively high signal-to-noise ratio).

5.1.1 Connection with convexity

In the context of stochastic optimization, i.e., minimizing $F(x) = \mathbf{E}_\xi[f(x, \xi)]$ with $g(x, \xi) = \nabla f(x, \xi)$, the classical aiming condition (31) is implied by F being μ -strongly convex and L -smooth [e.g., 36]. But in general it is a much weaker condition. Our aiming condition in Assumption A does not relate directly to smoothness and is not always implied by (strong) convexity either. However, it does have overlapping characteristics with convexity.

For ease of comparison, we consider the general block structure described in Section 1.3 with $d_t = \nabla f(x_t, \xi_t)$ and set $\lambda = 0$. In this case, we have $\mathbf{E}[d_t] = \nabla F(x_t)$ and

$$\sum_{k=1}^m \left\langle x_k - x_{*,k}, \frac{\nabla_k F(x)}{\sqrt{\mathbf{E}[\|\nabla_k f(x, \xi)\|^2]}} \right\rangle \geq 0, \quad \forall x, \quad (34)$$

where $\nabla_k F(x) \in \mathbf{R}^{n_k}$ denotes the sub-vector of $\nabla F(x)$ corresponding to the k th block. In the specific case of a full-dimensional block ($m = 1$), the denominator $\sqrt{\mathbf{E}[\|\nabla f(x, \xi)\|^2]}$ can be omitted without affecting the inequality and the aiming condition simplifies to:

$$\langle x - x_*, \nabla F(x) \rangle \geq 0, \quad \forall x. \quad (35)$$

This is a direct consequence of convexity, which is characterized by [e.g., 36]:

$$\langle x - y, \nabla F(x) - \nabla F(y) \rangle \geq 0, \quad \forall x, y.$$

To see the implication, simply substituting $y = x_*$ and $\nabla F(x_*) = 0$ into the above inequality gives the full-dimensional aiming condition.

However, other than the full-dimensional block case, the aiming condition (34) may exhibit significant departure from convexity. As an example, consider the case of single coordinate blocks with uniform SiF, i.e., $\rho_{t,k} = \rho_{t,k'}$ for all $k, k' \in \{1, \dots, n\}$. In light of the equivalent formulation using SiF in (33), the corresponding aiming condition becomes

$$\langle x - x_*, \text{sign}(\nabla F(x)) \rangle \geq 0, \quad \forall x. \quad (36)$$

Comparing this condition with convexity, it is easy to construct examples that satisfy one of them while failing the other. We provide some simple examples in Appendix B.1.

5.2 Analysis of conceptual BCOS

In this section, we provide convergence analysis for the conceptual BCOS method in (29). Our first result is about its one-step contraction property.

Lemma 5.1. *Suppose Assumption A holds, $\alpha_t \geq 0$ and $\alpha_t \lambda < 1$ for all $t \geq 0$. Then the sequence $\{x_t\}$ generated by (29) satisfies, for all $t \geq 0$,*

$$\mathbf{E}_t[\|x_{t+1} - x_*\|^2] \leq (1 - \alpha_t \lambda)^2 \|x_t - x_*\|^2 + \alpha_t^2 B_*, \quad (37)$$

where

$$B_* = n + \lambda^2 \|x_*\|^2 + 2\lambda \|x_*\|_1. \quad (38)$$

Proof. First, we notice that the aiming condition (32) is equivalent to

$$\left\langle x_t - x_*, \frac{\mathbf{E}_t[d_t]}{\sqrt{\mathbf{E}_t[d_t^2]}} + \lambda x_* \right\rangle \geq 0. \quad (39)$$

To see this, we simply add and subtract λx_t inside the inner product:

$$\begin{aligned} \left\langle x_t - x_*, \frac{\mathbf{E}_t[d_t]}{\sqrt{\mathbf{E}_t[d_t^2]}} + \lambda x_* \right\rangle &= \left\langle x_t - x_*, \frac{\mathbf{E}_t[d_t]}{\sqrt{\mathbf{E}_t[d_t^2]}} + \lambda x_t - \lambda x_t + \lambda x_* \right\rangle \\ &= \left\langle x_t - x_*, \frac{\mathbf{E}_t[d_t]}{\sqrt{\mathbf{E}_t[d_t^2]}} + \lambda x_t \right\rangle - \lambda \|x_t - x_*\|^2. \end{aligned}$$

Given $x_{t+1} = x_t - \tilde{\gamma}_t \odot d_t - \alpha_t x_t$, we have

$$\begin{aligned} \mathbf{E}_t[\|x_{t+1} - x_*\|^2] &= \mathbf{E}_t[\|x_t - \tilde{\gamma}_t \odot d_t - \alpha_t \lambda x_t - x_*\|^2] \\ &= \mathbf{E}_t[\|(1 - \alpha_t \lambda)x_t - \tilde{\gamma}_t \odot d_t - (1 - \alpha_t \lambda)x_* - \alpha_t \lambda x_*\|^2] \\ &= \mathbf{E}_t[\|(1 - \alpha_t \lambda)(x_t - x_*) - (\tilde{\gamma}_t \odot d_t + \alpha_t \lambda x_*)\|^2] \\ &= \mathbf{E}_t[\|(1 - \alpha_t \lambda)(x_t - x_*)\|^2] - 2\mathbf{E}_t[\langle (1 - \alpha_t \lambda)(x_t - x_*), \tilde{\gamma}_t \odot d_t + \alpha_t \lambda x_* \rangle] \\ &\quad + \mathbf{E}_t[\|\tilde{\gamma}_t \odot d_t + \alpha_t \lambda x_*\|^2]. \end{aligned} \quad (40)$$

We examine the three terms in the last equation one by one. Using the definition of $\mathbf{E}_t[\cdot]$, we can remove the conditional expectation from the first term, i.e.,

$$\mathbf{E}_t[\|(1 - \alpha_t \lambda)(x_t - x_*)\|^2] = \|(1 - \alpha_t \lambda)(x_t - x_*)\|^2 = (1 - \alpha_t \lambda)^2 \|x_t - x_*\|^2.$$

For the second term, we use $\tilde{\gamma}_t = \alpha_t / \sqrt{\mathbf{E}_t[d_t^2]}$ to obtain

$$\begin{aligned} \mathbf{E}_t[\langle (1 - \alpha_t \lambda)(x_t - x_*), \tilde{\gamma}_t \odot d_t + \alpha_t \lambda x_* \rangle] &= \langle (1 - \alpha_t \lambda)(x_t - x_*), \tilde{\gamma}_t \odot \mathbf{E}_t[d_t] + \alpha_t \lambda x_* \rangle \\ &= \alpha_t (1 - \alpha_t \lambda) \left\langle x_t - x_*, \frac{\mathbf{E}_t[d_t]}{\sqrt{\mathbf{E}_t[d_t^2]}} + \lambda x_* \right\rangle \\ &\geq 0, \end{aligned}$$

where the last inequality is due to (39). For the third term in (40), we have

$$\begin{aligned} \mathbf{E}_t[\|\tilde{\gamma}_t \odot d_t + \alpha_t \lambda x_*\|^2] &= \alpha_t^2 \mathbf{E}_t \left[\left\| \frac{d_t}{\sqrt{\mathbf{E}_t[d_t^2]}} + \lambda x_* \right\|^2 \right] \\ &= \alpha_t^2 \mathbf{E}_t \left[\sum_{k=1}^n \left(\frac{d_{t,k}^2}{\mathbf{E}_t[d_{t,k}^2]} + \lambda^2 x_{*,k}^2 + 2\lambda x_{*,k} \frac{d_{t,k}}{\sqrt{\mathbf{E}_t[d_{t,k}^2]}} \right) \right] \end{aligned}$$

$$\begin{aligned}
&= \alpha_t^2 \left[\sum_{k=1}^n \left(\frac{\mathbf{E}_t[d_{t,k}^2]}{\mathbf{E}_t[d_{t,k}^2]} + \lambda^2 x_{*,k}^2 + 2\lambda x_{*,k} \frac{\mathbf{E}[d_{t,k}]}{\sqrt{\mathbf{E}_t[d_{t,k}^2]}} \right) \right] \\
&= \alpha_t^2 \sum_{k=1}^n (1 + \lambda^2 x_{*,k}^2 + 2\lambda x_{*,k} \sqrt{\rho_{t,k}}) \\
&= \alpha_t^2 (n + \lambda^2 \|x_*\|^2 + 2\lambda \langle x_*, \sqrt{\rho_t} \rangle) \\
&\leq \alpha_t^2 (n + \lambda^2 \|x_*\|^2 + 2\lambda \|x_*\|_1 \|\sqrt{\rho_t}\|_\infty) \\
&\leq \alpha_t^2 (n + \lambda^2 \|x_*\|^2 + 2\lambda \|x_*\|_1),
\end{aligned}$$

where the last two inequalities are due to Hölder's inequality $\langle x_*, \sqrt{\rho_t} \rangle \leq \|x_*\|_1 \|\sqrt{\rho_t}\|_\infty$ and the fact that $\|\sqrt{\rho_t}\|_\infty \leq 1$, respectively. Plugging the above equality and inequalities into (40) yields the desired result. \square

As a direct consequence of Lemma 5.1, there exists sufficiently small $\alpha_t > 0$ such that

$$\mathbf{E}_t[\|x_{t+1} - x_*\|^2] \leq \|x_t - x_*\|^2, \quad \forall t \geq 0.$$

In fact, we can prove much stronger results, including almost sure convergence of x_t to x_* and characterizing the rate of convergence of $\mathbf{E}[\|x_t - x_*\|^2]$. These are presented in the following subsections.

5.2.1 Almost sure convergence

The following theorem establishes almost sure convergence of the conceptual BCOS algorithm under a classical condition on the sequence $\{\alpha_t\}$.

Theorem 5.1 (Almost sure convergence). *Suppose the stepsize schedule $\{\alpha_t\}_{t \geq 0}$ satisfies*

$$\alpha_t \geq 0, \quad \alpha_t \lambda \leq 1, \quad \forall t \geq 0, \quad \sum_{t=0}^{\infty} \alpha_t = \infty, \quad \sum_{t=0}^{\infty} \alpha_t^2 < \infty. \quad (41)$$

The under Assumption A, the sequence $\{x_t\}$ generated by (29) satisfies $\|x_t - x_\| \rightarrow 0$ a.s.*

The proof of Theorem 5.1 is based on the following *almost supermartingale* lemma of Robbins and Siegmund [43].

Lemma 5.2 (“Almost supermartingale”, [43, Theorem 1]). *Let (Ω, \mathcal{F}, P) be a probability space, and $\mathcal{F}_0 \subset \mathcal{F}_1 \subset \dots$ be a sequence of sub- σ -algebras of \mathcal{F} . For each $t \geq 0$, let X_t , a_t , b_t and c_t be non-negative \mathcal{F}_t -measurable random variables such that*

$$\mathbf{E}[X_{t+1} | \mathcal{F}_t] \leq X_t(1 + a_t) + b_t - c_t. \quad (42)$$

If $\sum_{t=0}^{\infty} a_t < \infty$ and $\sum_{t=0}^{\infty} b_t < \infty$, then $\lim_{t \rightarrow \infty} X_t$ exists and is finite, and $\sum_{t=0}^{\infty} c_t < \infty$ almost surely (a.s.).

Proof of Theorem 5.1. Define $X_t := \|x_t - x_*\|^2$ and \mathcal{F}_t to be the σ -algebra generated by X_0, \dots, X_t . Lemma 5.1 implies the following recursion, in the form of (42),

$$\begin{aligned}\mathbf{E}[X_{t+1}|\mathcal{F}_t] &\leq (1 - \alpha_t\lambda)^2 X_t + \alpha_t^2 B_* \\ &= (1 + \alpha_t^2\lambda^2) X_t + \alpha_t^2 B_* - 2\alpha_t\lambda X_t \\ &= (1 + a_t) X_t + b_t - c_t,\end{aligned}$$

where $a_t = \alpha_t^2\lambda^2$, $b_t = \alpha_t^2 B_*$ and $c_t = 2\alpha_t\lambda X_t$. Notice that X_t , a_t , b_t and c_t are all non-negative, and the square-summable assumption of α_t guarantees that

$$\sum_{t=0}^{\infty} a_t = \sum_{t=0}^{\infty} \alpha_t^2 \lambda^2 < \infty, \quad \sum_{t=0}^{\infty} b_t = \sum_{t=0}^{\infty} \alpha_t^2 B_* < \infty.$$

Therefore, all the assumptions in Lemma 5.2 are satisfied. We may now apply the lemma to conclude that $X_t = \|x_t - x_*\|^2 \rightarrow X$ for some $X < \infty$ and

$$\sum_{t=0}^{\infty} c_t = \sum_{t=0}^{\infty} 2\alpha_t\lambda \|x_t - x_*\|^2 < \infty \quad \text{a.s.}$$

This is compatible with the assumption $\sum_{t=0}^{\infty} \alpha_t = \infty$ only if $\|x_t - x_*\|^2 \rightarrow 0$ a.s. \square

5.2.2 Rates of convergence

First, with a constant stepsize schedule, we have linear convergence to a neighborhood of x_* as stated by the following corollary.

Corollary 5.1. *Consider the conceptual BCOS method (29) and fix the stepsize schedule $\alpha_t = \alpha$ where α satisfies $\alpha\lambda < 1$. Then under Assumption A, we have*

$$\mathbf{E}[\|x_t - x_*\|^2] \leq (1 - \alpha\lambda)^{2t} \mathbf{E}[\|x_0 - x_*\|^2] + \frac{\alpha^2 B_*}{1 - (1 - \alpha\lambda)^2},$$

where B_* is defined in (38).

Proof. Recursive application of Lemma 5.1 with $\alpha_t = \alpha$ yields

$$\begin{aligned}\mathbf{E}[\|x_t - x_*\|^2] &\leq (1 - \alpha\lambda)^{2t} \mathbf{E}[\|x_0 - x_*\|^2] + \sum_{s=0}^{t-1} (1 - \alpha\lambda)^{2(t-s-1)} \alpha^2 B_* \\ &= (1 - \alpha\lambda)^{2t} \mathbf{E}[\|x_0 - x_*\|^2] + \sum_{s=0}^{t-1} (1 - \alpha\lambda)^{2s} \alpha^2 B_* \\ &\leq (1 - \alpha\lambda)^{2t} \mathbf{E}[\|x_0 - x_*\|^2] + \frac{\alpha^2 B_*}{1 - (1 - \alpha\lambda)^2},\end{aligned}$$

which is the desired result. \square

With a diminishing stepsize schedule α_t , we can show that $\mathbf{E}[\|x_t - x_*\|^2] \rightarrow 0$ at a sublinear rate, as given in the following theorem.

Theorem 5.2. *Consider the algorithm (29) with stepsize schedule $\alpha_t = \frac{\alpha}{t+1}$. Suppose the constant α satisfies $1/2 < \alpha\lambda < 1$ and Assumption A holds. Then we have for all $t \geq 0$,*

$$\mathbf{E}[\|x_t - x_*\|^2] \leq \frac{\alpha^2 (\lambda^2 \mathbf{E}[\|x_0 - x_*\|^2] + (1 + \pi^2/6)B_*)}{2\alpha\lambda - 1} \frac{1}{t+1} + \mathcal{O}\left(\frac{1}{(t+1)^2} + \frac{1}{(t+1)^{2\alpha\lambda}}\right),$$

where B_* is defined in (38).

Our proof of Theorem 5.2 is based on Lemma 5.1 and a classical result of Chung [7].

Lemma 5.3 (Chung's lemma, [7, Lemma 1]). *Suppose that $\{X_t\}$ is a sequence of real numbers such that for all $t \geq 1$,*

$$X_{t+1} \leq \left(1 - \frac{a}{t}\right) X_t + \frac{b}{t^{p+1}}, \quad (43)$$

where $a > p > 0$ and $b > 0$. Then

$$X_t \leq \frac{b}{a-p} \frac{1}{t^p} + \mathcal{O}\left(\frac{1}{t^{p+1}} + \frac{1}{t^a}\right).$$

In order to apply Chung's lemma, we need to first derive an upper bound on $\mathbf{E}[\|x_t - x_*\|^2]$ for any $t \geq 0$, which will be incorporated into the constant b in the lemma. To this end, we start with the inequality (37) and use the law of total expectation to get

$$\begin{aligned} \mathbf{E}[\|x_t - x_*\|^2] &= \mathbf{E}[\mathbf{E}_{t-1}[\|x_t - x_*\|^2]] \\ &\leq \mathbf{E}[(1 - \alpha_{t-1}\lambda)^2 \|x_{t-1} - x_*\|^2 + \alpha_{t-1}^2 B_*] \\ &\leq \mathbf{E}[\|x_{t-1} - x_*\|^2] + \alpha_{t-1}^2 B_* \\ &\leq \mathbf{E}[\|x_0 - x_*\|^2] + B_* \sum_{s=0}^{t-1} \alpha_s^2, \end{aligned} \quad (44)$$

where the last term is bounded if $\sum_{t=1}^{\infty} \alpha_t^2 < \infty$.

Proof of Theorem 5.2. Taking total expectation on both sides of (37), we obtain

$$\begin{aligned} \mathbf{E}[\|x_{t+1} - x_*\|^2] &\leq (1 - \alpha_t\lambda)^2 \mathbf{E}[\|x_t - x_*\|^2] + \alpha_t^2 B_* \\ &= (1 - 2\alpha_t\lambda) \mathbf{E}[\|x_t - x_*\|^2] + \alpha_t^2 (\lambda^2 \mathbf{E}[\|x_t - x_*\|^2] + B_*). \end{aligned} \quad (45)$$

We bound $\mathbf{E}[\|x_t - x_*\|^2]$ by substituting $\alpha_t = \frac{\alpha}{t+1}$ into (44), which leads to

$$\begin{aligned} \mathbf{E}[\|x_t - x_*\|^2] &\leq \mathbf{E}[\|x_0 - x_*\|^2] + B_* \sum_{s=0}^{\infty} \frac{\alpha^2}{(s+1)^2} \\ &= \mathbf{E}[\|x_0 - x_*\|^2] + \frac{\pi^2}{6} \alpha^2 B_*. \end{aligned}$$

Applying the above bound to the last term of (45) and setting $\alpha_t = \frac{\alpha}{t+1}$, we get

$$\begin{aligned}\mathbf{E}[\|x_{t+1} - x_*\|^2] &\leq \left(1 - \frac{2\alpha\lambda}{t+1}\right) \mathbf{E}[\|x_t - x_*\|^2] + \frac{\alpha^2(\lambda^2\mathbf{E}[\|x_0 - x_*\|^2] + (\pi^2/6)\alpha^2\lambda^2 B_* + B_*)}{(t+1)^2} \\ &\leq \left(1 - \frac{2\alpha\lambda}{t+1}\right) \mathbf{E}[\|x_t - x_*\|^2] + \frac{\alpha^2(\lambda^2\mathbf{E}[\|x_0 - x_*\|^2] + (1 + \pi^2/6)B_*)}{(t+1)^2},\end{aligned}$$

where in the second inequality we used the assumption $\alpha\lambda < 1$.

Let $X_{t+1} = \mathbf{E}[\|x_t - x_*\|^2]$, $a = 2\alpha\lambda$, $p = 1$ and $b = \alpha^2(\lambda^2\mathbf{E}[\|x_0 - x_*\|^2] + (1 + \pi^2/6)B_*)$. Then the above inequality can be written as

$$X_{t+2} \leq \left(1 - \frac{a}{t+1}\right) X_{t+1} + \frac{b}{(t+1)^{p+1}},$$

which is in the form of (43) except with the index shift $t \rightarrow t+1$. Applying Lemma 5.3 gives the desired result. \square

Theorem 5.2 requires $\alpha\lambda > 1/2$ to obtain the $\mathcal{O}(1/t)$ rate of convergence. We can remove this condition by working with the stepsize schedule $\alpha_t = \frac{\alpha}{(t+1)^p}$ with $p \in (\frac{1}{2}, 1)$. In this case we have an *asymptotic* $\mathcal{O}(1/t^p)$ rate, as stated in the following theorem.

Theorem 5.3. *Consider the algorithm (29) with stepsize schedule $\alpha_t = \frac{\alpha}{(t+1)^p}$ where $p \in (\frac{1}{2}, 1)$ and the constant α satisfies $\alpha\lambda < 1$. Then under Assumption A, we have*

$$\limsup_{t \rightarrow \infty} (t+1)^p \mathbf{E}[\|x_t - x_*\|^2] \leq \frac{\alpha(\lambda^2\mathbf{E}[\|x_0 - x_*\|^2] + (1 + K_p)B_*)}{2\lambda}, \quad (46)$$

where $K_p = \sum_{t=1}^{\infty} \frac{1}{(t+1)^{2p}}$ is finite for $p \in (\frac{1}{2}, 1)$.

The proof is based on another lemma of Chung [7], restated below.

Lemma 5.4 ([7, Lemma 4]). *Suppose that $\{X_t\}$ is a sequence of real numbers such that for all $t \geq 1$,*

$$X_{t+1} \leq \left(1 - \frac{a_t}{t^p}\right) X_t + \frac{b}{t^q}, \quad (47)$$

where $0 < p < 1, p < q, a_t \geq a > 0, b > 0$. Then

$$\limsup_{t \rightarrow \infty} t^{q-p} X_t \leq \frac{b}{a}.$$

Proof of Theorem 5.3. Substituting $\alpha_t = \frac{\alpha}{(t+1)^p}$ into (44), we obtain

$$\mathbf{E}[\|x_t - x_*\|^2] \leq \mathbf{E}[\|x_0 - x_*\|^2] + B_* \sum_{s=0}^{\infty} \frac{\alpha^2}{(s+1)^{2p}} = \mathbf{E}[\|x_0 - x_*\|^2] + K_p \alpha^2 B_*.$$

Taking total expectation of both sides of (37) and plugging in $\alpha_t = \frac{\alpha}{(t+1)^p}$, we get

$$\begin{aligned}\mathbf{E}[\|x_{t+1} - x_*\|^2] &\leq (1 - \alpha_t \lambda)^2 \mathbf{E}[\|x_t - x_*\|^2] + \alpha_t^2 B_* \\ &= (1 - 2\alpha_t \lambda) \mathbf{E}[\|x_t - x_*\|^2] + \alpha_t^2 (B_* + \lambda^2 \mathbf{E}[\|x_t - x_*\|^2]) \\ &\leq \left(1 - \frac{2\alpha \lambda}{(t+1)^p}\right) \mathbf{E}[\|x_t - x_*\|^2] + \frac{\alpha^2 (\lambda^2 \mathbf{E}[\|x_0 - x_*\|^2] + (1 + K_p) B_*)}{(t+1)^{2p}}.\end{aligned}$$

The desired result follows by applying Lemma 5.4 with the definitions $X_{t+1} = \mathbf{E}[\|x_t - x_*\|^2]$, $a_t = a = 2\alpha \lambda$, $b = \alpha^2 (\lambda^2 \mathbf{E}[\|x_0 - x_*\|^2] + (1 + K_p) B_*)$ and $q = 2p$. \square

5.2.3 Analysis for not using decoupled weight decay

Here we briefly explain the convergence analysis of BCOS in the case of $\lambda = 0$, or in the case of $\lambda > 0$ but without using decoupled weight decay. In other words, we consider

$$x_{t+1} = x_t - \tilde{\gamma}_t \odot d_t = x_t - \alpha_t \frac{d_t}{\sqrt{\mathbf{E}_t[d_t^2]}}. \quad (48)$$

The aiming condition (32) becomes

$$\left\langle x_t - x_*, \frac{\mathbf{E}_t[d_t]}{\sqrt{\mathbf{E}_t[d_t^2]}} \right\rangle \geq 0. \quad (49)$$

In order to establish similar convergence guarantees as before, we need slightly stronger aiming conditions, as discussed below.

1. First, with $\lambda = 0$, we have the following inequality in place of (37) (see Lemma 5.1):

$$\mathbf{E}_t[\|x_{t+1} - x_*\|^2] \leq \|x_t - x_*\|^2 - \alpha_t \left\langle x_t - x_*, \frac{\mathbf{E}_t[d_t]}{\sqrt{\mathbf{E}_t[d_t^2]}} \right\rangle + \alpha_t^2 n.$$

To have contraction with sufficiently small α_t , we need the aiming condition (49) to hold with strict inequality for any $x_t \neq x_*$.

2. Almost sure convergence as in Theorem 5.4 requires a slightly stronger condition

$$\left\langle x_t - x_*, \frac{\mathbf{E}_t[d_t]}{\sqrt{\mathbf{E}_t[d_t^2]}} \right\rangle \geq \phi(\|x_t - x_*\|),$$

where ϕ is any strictly positive and continuous function.

3. To obtain sublinear rates of convergence as in Theorems 5.2 and 5.3, we need an even stronger aiming condition, specifically,

$$\left\langle x_t - x_*, \frac{\mathbf{E}_t[d_t]}{\sqrt{\mathbf{E}_t[d_t^2]}} \right\rangle \geq \mu \|x_t - x_*\|^2, \quad (50)$$

with some $\mu > 0$ for all $t \geq 0$.

Finally, we comment on the case of adding the regularization $(\lambda/2)\|x\|^2$ with $\lambda > 0$ but *without* using decoupled weight-decay. Specifically, we compute $g_t = \nabla f(x_t, \xi_t) + \lambda x_t$ with $\lambda > 0$ and apply the BCOS method (48) with d_t being g_t or its EMA. It is worth emphasizing that, in this case, the aiming condition (50) does *not* automatically hold with $\mu = \lambda$. This has to do with the coordinate-wise scaling of d_t by $\sqrt{\mathbf{E}_t[d_t]}$. To see this, we consider the loss function $F(x)$ defined in (27), i.e.,

$$F(x) := \mathbf{E}_\xi[f(x, \xi)] + \frac{\lambda}{2}\|x\|^2,$$

and assume that $\mathbf{E}_\xi[f(x, \xi)]$ is convex. We contrast the two cases discussed in Section 5.1.1.

- With full coordinate block, it is straightforward to show that under the convex assumption, the aiming condition (35) is strengthened to

$$\langle x - x_*, \nabla F(x) \rangle \geq \lambda \|x - x_*\|^2.$$

- However, the above argument does not extend to the case with coordinate-wise scaling. As an example, consider the special case of having uniform SiF across all coordinates. In this case, the corresponding aiming condition (36) *cannot* be strengthened to

$$\langle x - x_*, \text{sign}(\nabla F(x)) \rangle \geq \lambda \|x - x_*\|^2,$$

because the $\text{sign}(\cdot)$ function is indifferent or insensitive to the curvature brought by the regularization $(\lambda/2)\|x\|^2$. In general, with coordinate-wise scaling and nonuniform SiF, the condition (50) may hold with some positive μ that is much smaller than λ .

The above discussion gives a plausible explanation to the empirical observation that decoupled weight decay works better for methods with coordinate-wise scaling (e.g., see Figure 3).

5.3 Analysis for practical BCOS

In this section, we provide convergence analysis for the practical BCOS method

$$x_{t+1} = (1 - \alpha_t \lambda) x_t - \alpha_t \frac{d_t}{\sqrt{v_t + \epsilon}}, \quad (51)$$

where v_t is an online estimator of the conditional second moment $\mathbf{E}_t[d_t^2]$. As explained at the beginning of Section 5, our analysis is based on bounding the difference between the expected steps under the practical method and the conceptual method, in the form of (30). To proceed, we first decompose their difference into two terms, i.e.,

$$\left| \frac{\mathbf{E}_t[d_t]}{\sqrt{\mathbf{E}[d_t^2]}} - \mathbf{E}_t \left[\frac{d_t}{\sqrt{v_t + \epsilon}} \right] \right| \leq \left| \frac{\mathbf{E}_t[d_t]}{\sqrt{\mathbf{E}[d_t^2]}} - \frac{\mathbf{E}_t[d_t]}{\sqrt{\mathbf{E}_t[v_t] + \epsilon}} \right| + \left| \frac{\mathbf{E}_t[d_t]}{\sqrt{\mathbf{E}_t[v_t] + \epsilon}} - \mathbf{E}_t \left[\frac{d_t}{\sqrt{v_t + \epsilon}} \right] \right|, \quad (52)$$

and then bound the two error terms on the right-hand side separately. Intuitively, the magnitudes of these two error terms are determined by the quality of the estimator v_t . We make the following assumption on the bias of v_t .

Assumption B (Bias of second-moment estimator). *There exists $\tau \in (0, 1)$ and $\epsilon > 0$ such that for all $t \geq 0$,*

$$|\mathbf{E}_t[v_t] - \mathbf{E}_t[d_t^2]| \leq \tau \mathbf{E}_t[d_t^2] + \epsilon. \quad (53)$$

Here ϵ is an additive error bound that leaves room for $\mathbf{E}_t[v_t]$ when $\mathbf{E}_t[d_t^2]$ is very small. There is no loss of generality by restricting $\tau < 1$ in the sense that we can always find an estimator that satisfies the assumption with sufficiently large ϵ . As an extreme case, by setting $\epsilon \geq \|\mathbf{E}_t[d_t^2]\|_\infty$ for all t , the trivial estimator $v_t = 0$ satisfies (53) for any $\tau \in (0, 1)$.

5.3.1 Bounding the difference between conceptual and practical BCOS updates

The following lemma derives an upper bound on the first term on the right-hand side of (52). The proof is given in Appendix B.2.

Lemma 5.5. *Under Assumption B, it holds that:*

$$\left| \frac{\mathbf{E}_t[d_t]}{\sqrt{\mathbf{E}_t[d_t^2]}} - \frac{\mathbf{E}_t[d_t]}{\sqrt{\mathbf{E}_t[v_t] + \epsilon}} \right| \leq \frac{\tau + \mathcal{O}(\tau^2)}{2} \left| \frac{\mathbf{E}_t[d_t]}{\sqrt{\mathbf{E}_t[d_t^2]}} \right| + \mathcal{O}(\epsilon). \quad (54)$$

To bound the second term on the right-hand side of (52), we need the following lemma, whose proof is given in Appendix B.3.

Lemma 5.6. *Let Y, Z be two random variables and $Z > 0$ almost surely, then*

$$\mathbf{E} \left[\frac{Y}{\sqrt{Z}} \right] = \frac{\mathbf{E}[Y]}{\sqrt{\mathbf{E}[Z]}} \left(1 - \frac{\text{Cov}(Y, Z)}{2\mathbf{E}[Y]\mathbf{E}[Z]} + \frac{3\text{Var}(Z)}{8\mathbf{E}[Z]^2} + \mathcal{O} \left(\frac{\text{Var}(Z)}{\mathbf{E}[Z]^2} \right) \right) \quad (55)$$

where $\mathcal{O} \left(\frac{\text{Var}(Z)}{\mathbf{E}[Z]^2} \right)$ includes higher-order statistical terms

$$\frac{\mathbf{E}[(Y - \mathbf{E}[Y])(Z - \mathbf{E}[Z])^{p-1}]}{\mathbf{E}[Y]\mathbf{E}[Z]^{p-1}} \quad \text{and} \quad \frac{\mathbf{E}[(Z - \mathbf{E}[Z])^p]}{\mathbf{E}[Z]^p},$$

for $p \geq 3$.

Applying Lemma 5.6 with $Y = d_t$ and $Z = v_t + \epsilon$, we get the coordinate-wise inequality

$$\left| \frac{\mathbf{E}_t[d_t]}{\sqrt{\mathbf{E}_t[v_t] + \epsilon}} - \mathbf{E}_t \left[\frac{d_t}{\sqrt{v_t + \epsilon}} \right] \right| \leq \left| \frac{\mathbf{E}_t[d_t]}{\sqrt{\mathbf{E}_t[v_t] + \epsilon}} \right| \odot \left| \frac{-\text{Cov}_t(d_t, v_t + \epsilon)}{2\mathbf{E}_t[d_t]\mathbf{E}_t[v_t + \epsilon]} + \mathcal{O} \left(\frac{\text{Var}_t(v_t + \epsilon)}{\mathbf{E}_t[v_t + \epsilon]^2} \right) \right|. \quad (56)$$

In order to gain more intuition, we express the above bound using the conditional *signal-to-noise ratio* (SNR) of d_t and $v_t + \epsilon$, defined as

$$\text{SNR}_t(d_t) = \frac{\mathbf{E}_t[d_t]^2}{\text{Var}_t(d_t)}, \quad \text{SNR}_t(v_t + \epsilon) = \frac{\mathbf{E}_t[v_t + \epsilon]^2}{\text{Var}_t(v_t + \epsilon)} = \frac{\mathbf{E}_t[v_t + \epsilon]^2}{\text{Var}_t(v_t)}.$$

With the definition of SNRs, the term containing $\text{Cov}_t(d_t, v_t + \epsilon)$ in (56) can be expressed as

$$\begin{aligned} \frac{\text{Cov}_t(d_t, v_t + \epsilon)}{\mathbf{E}_t[d_t]\mathbf{E}_t[v_t + \epsilon]} &= \frac{\text{Cov}_t(d_t, v_t)}{\mathbf{E}_t[d_t]\mathbf{E}_t[v_t + \epsilon]} \\ &= \frac{\text{Cov}_t(d_t, v_t)}{\sqrt{\text{Var}_t(d_t)\text{Var}_t(v_t)}} \sqrt{\frac{\text{Var}_t(d_t)\text{Var}_t(v_t)}{\mathbf{E}_t[d_t]^2\mathbf{E}_t[v_t + \epsilon]^2}} \\ &= \text{Corr}_t(d_t, v_t) \frac{1}{\sqrt{\text{SNR}_t(d_t)\text{SNR}_t(v_t + \epsilon)}}, \end{aligned}$$

where we use the definition of correlation of two random variables: $\text{Corr}(Y, Z) = \frac{\text{Cov}(Y, Z)}{\sqrt{\text{Var}(Y)\text{Var}(Z)}}$.

Substituting the expressions using SNRs into (56), we obtain

$$\left| \frac{\mathbf{E}_t[d_t]}{\sqrt{\mathbf{E}_t[v_t] + \epsilon}} - \mathbf{E}_t \left[\frac{d_t}{\sqrt{v_t + \epsilon}} \right] \right| \leq \left| \frac{\mathbf{E}_t[d_t]}{\sqrt{\mathbf{E}_t[v_t] + \epsilon}} \right| \odot \left| \frac{-(1/2)\text{Corr}_t(d_t, v_t)}{\sqrt{\text{SNR}_t(d_t)\text{SNR}_t(v_t + \epsilon)}} + \mathcal{O}\left(\frac{1}{\text{SNR}_t(v_t + \epsilon)}\right) \right|.$$

We are ready to bound the difference between the expected updates of the practical BCOS and the conceptual BCOS methods. Specifically, bounding the first term on the right-hand side of (52) using Lemma 5.5 and the second term using the last inequality above, we obtain

$$\begin{aligned} \left| \frac{\mathbf{E}_t[d_t]}{\sqrt{\mathbf{E}_t[d_t^2]}} - \mathbf{E}_t \left[\frac{d_t}{\sqrt{v_t + \epsilon}} \right] \right| &\leq \frac{\tau + \mathcal{O}(\tau^2)}{2} \left| \frac{\mathbf{E}_t[d_t]}{\sqrt{\mathbf{E}_t[d_t^2]}} \right| + \mathcal{O}(\epsilon) \\ &\quad + \left| \frac{\mathbf{E}_t[d_t]}{\sqrt{v_t + \epsilon}} \right| \odot \left| \frac{-(1/2)\text{Corr}_t(d_t, v_t)}{\sqrt{\text{SNR}_t(d_t)\text{SNR}_t(v_t + \epsilon)}} + \mathcal{O}\left(\frac{1}{\text{SNR}_t(v_t + \epsilon)}\right) \right|. \end{aligned}$$

We can further merge the two terms on the right-hand side by bounding $\left| \frac{\mathbf{E}_t[d_t]}{\sqrt{v_t + \epsilon}} \right|$ in terms of $\left| \frac{\mathbf{E}_t[d_t]}{\sqrt{\mathbf{E}_t[d_t^2]}} \right|$. To this end, we use Lemma 5.5 to obtain

$$\left| \frac{\mathbf{E}_t[d_t]}{\sqrt{\mathbf{E}_t[v_t] + \epsilon}} \right| \leq \left(1 + \frac{\tau + \mathcal{O}(\tau^2)}{2} \right) \left| \frac{\mathbf{E}_t[d_t]}{\sqrt{\mathbf{E}_t[d_t^2]}} \right| + \mathcal{O}(\epsilon).$$

Combining the two inequalities above, we arrive at the following result.

Lemma 5.7. *Under Assumptions B, we have for all $t \geq 0$,*

$$\left| \mathbf{E}_t \left[\frac{d_t}{\sqrt{v_t + \epsilon}} \right] - \frac{\mathbf{E}_t[d_t]}{\sqrt{\mathbf{E}_t[d_t^2]}} \right| \leq \sigma_t \left| \frac{\mathbf{E}_t[d_t]}{\sqrt{\mathbf{E}_t[d_t^2]}} \right| + \mathcal{O}(\epsilon),$$

where

$$\sigma_t = \frac{\tau + \mathcal{O}(\tau^2)}{2} + \left(1 + \frac{\tau + \mathcal{O}(\tau^2)}{2} \right) \left\| \frac{-(1/2)\text{Corr}_t(d_t, v_t)}{\sqrt{\text{SNR}_t(d_t)\text{SNR}_t(v_t + \epsilon)}} + \mathcal{O}\left(\frac{1}{\text{SNR}_t(v_t + \epsilon)}\right) \right\|_{\infty}. \quad (57)$$

5.3.2 Almost sure convergence of practical BCOS

The following lemma is a variant of the aiming condition with the practical BCOS update.

Lemma 5.8. *Under Assumptions B, it holds that*

$$\left\langle x_t - x_*, \mathbf{E}_t \left[\frac{d_t}{\sqrt{v_t + \epsilon}} \right] \right\rangle \geq \left\langle x_t - x_*, \frac{\mathbf{E}_t[d_t]}{\sqrt{\mathbf{E}_t[d_t^2]}} \right\rangle - \|x_t - x_*\|_1 (\sigma_t + \mathcal{O}(\epsilon)), \quad (58)$$

where σ_t is given by (57).

Proof. Adding and subtracting the term $\frac{\mathbf{E}_t[d_t]}{\sqrt{\mathbf{E}_t[d_t^2]}}$ from the inner product, we obtain:

$$\begin{aligned} & \left\langle x_t - x_*, \mathbf{E}_t \left[\frac{d_t}{\sqrt{v_t + \epsilon}} \right] \right\rangle \\ &= \left\langle x_t - x_*, \frac{\mathbf{E}_t[d_t]}{\sqrt{\mathbf{E}_t[d_t^2]}} \right\rangle + \left\langle x_t - x_*, \mathbf{E}_t \left[\frac{d_t}{\sqrt{v_t + \epsilon}} \right] - \frac{\mathbf{E}_t[d_t]}{\sqrt{\mathbf{E}_t[d_t^2]}} \right\rangle \\ &\geq \left\langle x_t - x_*, \frac{\mathbf{E}_t[d_t]}{\sqrt{\mathbf{E}_t[d_t^2]}} \right\rangle - \|x_t - x_*\|_1 \cdot \left\| \mathbf{E}_t \left[\frac{d_t}{\sqrt{v_t + \epsilon}} \right] - \frac{\mathbf{E}_t[d_t]}{\sqrt{\mathbf{E}_t[d_t^2]}} \right\|_\infty \\ &\geq \left\langle x_t - x_*, \frac{\mathbf{E}_t[d_t]}{\sqrt{\mathbf{E}_t[d_t^2]}} \right\rangle - \|x_t - x_*\|_1 \left(\sigma_t \left\| \frac{\mathbf{E}_t[d_t]}{\sqrt{\mathbf{E}_t[d_t^2]}} \right\|_\infty + \mathcal{O}(\epsilon) \right), \end{aligned}$$

where the first inequality is due to Hölder's inequality and the last inequality is due to Lemma 5.7. In addition, we notice that

$$\left\| \frac{\mathbf{E}_t[d_t]}{\sqrt{\mathbf{E}_t[d_t^2]}} \right\|_\infty = \|\sqrt{\rho_t}\|_\infty \leq 1, \quad (59)$$

which concludes the proof. \square

Theorem 5.4 (Almost sure convergence of BCOSW). *Consider the practical BCOSW method (28). Suppose that Assumptions A and B hold, d_t is bounded almost surely, and $\{\alpha_t\}$ satisfies (41). Then there exists $\delta > 0$ such that we have with probability one,*

$$\limsup_{t \rightarrow \infty} \|x_t - x_*\|^2 \leq \delta^2. \quad (60)$$

More specifically, δ is the smallest constant such that $\|x - x_*\| \geq \delta$ implies

$$2\|x - x_*\|_1 (\sigma_t + \mathcal{O}(\epsilon)) \leq \lambda \|x - x_*\|^2, \quad \forall t \geq 0, \quad (61)$$

where σ_t is given by (57).

The proof of Theorem 5.4 is based on a classical result of stochastic approximation due to Dvoretzky [12]. Here we present an extension that best fits our purpose.

Theorem 5.5 (An extension of Dvoretzky's Theorem). *Let $(\Omega = \{\omega\}, \mathcal{F}, P)$ be a probability space. Let $\{x_t\}$ and $\{y_t\}$ be sequences of random variables such that, for all $t \geq 0$,*

$$x_{t+1}(\omega) = T_t(x_0(\omega), \dots, x_t(\omega)) + y_t(\omega), \quad (62)$$

where the transformation T_t satisfy, for any $x_0, \dots, x_t \in \mathbf{R}^n$,

$$\|T_t(x_0, \dots, x_t) - x_*\|^2 \leq \max\{a_t, (1 + b_t)\|x_t - x_*\|^2 - c_t + h_t\}, \quad (63)$$

and the sequences $\{a_t\}$, $\{b_t\}$, $\{c_t\}$ and $\{h_t\}$ are non-negative and satisfy

$$\lim_{t \rightarrow \infty} a_t = a_\infty, \quad \sum_{t=0}^{\infty} b_t < \infty, \quad \sum_{t=0}^{\infty} c_t = \infty, \quad \sum_{t=1}^{\infty} h_t < \infty. \quad (64)$$

In addition, suppose the following conditions hold with probability one:

$$\mathbf{E}[\|x_0\|^2] < \infty, \quad \sum_{t=0}^{\infty} \mathbf{E}[\|y_t\|^2] < \infty, \quad \mathbf{E}[y_t | x_0, \dots, x_t] = 0 \quad \forall t \geq 0. \quad (65)$$

Then we have with probability one,

$$\limsup_{t \rightarrow \infty} \|x_t - x_*\|^2 \leq a_\infty.$$

Remark. There are many extensions of Dvoretzky's original results [15]. Theorem 5.5 is a minor variation of Venter [53, Theorem 1]. More concretely,

- Theorem 1 of Venter [53] has the sequence $\{a_t\}$ being a constant sequence, i.e., $a_t = a_\infty$ for all $t \geq 0$. The extension to a non-constant sequence $\{a_t\}$ is outlined in the original work of Dvoretzky [15] and admits a simple proof due to Derman and Sacks [12].
- Theorem 1 of Venter [53] does not include the sequence $\{h_t\}$. The extension with $\sum_{t=0}^{\infty} h_t < \infty$ is straightforward based on a simple argument of Dvoretzky [15].
- More generally, the sequences $\{a_t\}$, $\{b_t\}$, $\{c_t\}$, $\{h_t\}$ can be non-negative measurable functions of x_0, \dots, x_t , and the conclusion of Theorem 5.5 holds if a_∞ is an upper bound on $\limsup_{t \rightarrow \infty} a_t(x_0, \dots, x_t)$ uniformly for all sequences $\{x_t\}$ [12, 43].

Proof of Theorem 5.5. We first write the practical BCOSW algorithm in the form of (62):

$$\begin{aligned} x_{t+1} &= (1 - \alpha_t \lambda) x_t - \alpha_t \frac{d_t}{\sqrt{v_t + \epsilon}} \\ &= (1 - \alpha_t \lambda) x_t - \alpha_t \mathbf{E}_t \left[\frac{d_t}{\sqrt{v_t + \epsilon}} \right] + \alpha_t \left(\mathbf{E}_t \left[\frac{d_t}{\sqrt{v_t + \epsilon}} \right] - \frac{d_t}{\sqrt{v_t + \epsilon}} \right). \end{aligned}$$

Thus we have $x_{t+1} = T_t(x_0, \dots, x_t) + y_t$ with

$$\begin{aligned} T_t(x_0, \dots, x_t) &= (1 - \alpha_t \lambda) x_t - \alpha_t \mathbf{E}_t \left[\frac{d_t}{\sqrt{v_t + \epsilon}} \right], \\ y_t &= \alpha_t \left(\mathbf{E}_t \left[\frac{d_t}{\sqrt{v_t + \epsilon}} \right] - \frac{d_t}{\sqrt{v_t + \epsilon}} \right). \end{aligned}$$

Apparently $\mathbf{E}_t[y_t] = \mathbf{E}[y_t|x_0, \dots, x_t] = 0$. We also have $\sum_{t=0}^{\infty} \mathbf{E}[\|y_t\|^2] < \infty$ due to the assumptions that $\sum_{t=0}^{\infty} \alpha_t^2 < \infty$ and d_t is bounded almost surely. Therefore the conditions in (65) are all satisfied.

The squared distance between $T_t(x_0, \dots, x_t)$ and x_* admits the following expansion:

$$\begin{aligned} \|T_t(x_0, \dots, x_t) - x_*\|^2 &= \left\| (1 - \alpha_t \lambda) x_t - \alpha_t \mathbf{E}_t \left[\frac{d_t}{\sqrt{v_t + \epsilon}} \right] - x_* \right\|^2 \\ &= \left\| (1 - \alpha_t \lambda)(x_t - x_*) - \alpha_t \left(\mathbf{E}_t \left[\frac{d_t}{\sqrt{v_t + \epsilon}} \right] + \lambda x_* \right) \right\|^2 \\ &= (1 - \alpha_t \lambda)^2 \|x_t - x_*\|^2 - 2\alpha_t(1 - \alpha_t \lambda) \left\langle x_t - x_*, \mathbf{E}_t \left[\frac{d_t}{\sqrt{v_t + \epsilon}} \right] + \lambda x_* \right\rangle \\ &\quad + \alpha_t^2 \left\| \mathbf{E}_t \left[\frac{d_t}{\sqrt{v_t + \epsilon}} \right] + \lambda x_* \right\|^2. \end{aligned}$$

Using Lemma 5.8 and then the aiming condition (39), we obtain

$$\begin{aligned} \left\langle x_t - x_*, \mathbf{E}_t \left[\frac{d_t}{\sqrt{v_t + \epsilon}} \right] + \lambda x_* \right\rangle &\geq \left\langle x_t - x_*, \frac{\mathbf{E}_t[d_t]}{\sqrt{\mathbf{E}_t[d_t^2]}} + \lambda x_* \right\rangle - \|x_t - x_*\|_1 (\sigma_t + \mathcal{O}(\epsilon)) \\ &\geq -\|x_t - x_*\|_1 (\sigma_t + \mathcal{O}(\epsilon)). \end{aligned}$$

By the assumption that d_t is bounded almost surely, there exists a constant B such that

$$\left\| \mathbf{E}_t \left[\frac{d_t}{\sqrt{v_t + \epsilon}} \right] + \lambda x_* \right\|^2 \leq B, \quad \forall t \geq 0.$$

Together with $0 < 1 - \alpha_t \lambda < 1$, we conclude that

$$\begin{aligned} \|T_t(x_0, \dots, x_t) - x_*\|^2 &\leq (1 - \alpha_t \lambda)^2 \|x_t - x_*\|^2 + 2\alpha_t(1 - \alpha_t \lambda) \|x_t - x_*\|_1 (\sigma_t + \mathcal{O}(\epsilon)) + \alpha_t^2 B \\ &\leq (1 - \alpha_t \lambda)^2 \|x_t - x_*\|^2 + 2\alpha_t \|x_t - x_*\|_1 (\sigma_t + \mathcal{O}(\epsilon)) + \alpha_t^2 B \\ &= (1 + \alpha_t^2 \lambda^2) \|x_t - x_*\|^2 - 2\alpha_t \lambda \|x_t - x_*\|^2 + 2\alpha_t \|x_t - x_*\|_1 (\sigma_t + \mathcal{O}(\epsilon)) \\ &\quad + \alpha_t^2 B \\ &= (1 + \alpha_t^2 \lambda^2) \|x_t - x_*\|^2 + \alpha_t (2\|x_t - x_*\|_1 (\sigma_t + \mathcal{O}(\epsilon)) - \lambda \|x_t - x_*\|^2) \\ &\quad - \alpha_t \lambda \|x_t - x_*\|^2 + \alpha_t^2 B. \end{aligned} \tag{66}$$

We observe that there exist $\delta > 0$ such that for all $t \geq 0$,

$$\|x_t - x_*\| \geq \delta \implies 2\|x_t - x_*\|_1(\sigma_t + \mathcal{O}(\epsilon)) - \lambda\|x_t - x_*\|^2 \leq 0.$$

Therefore, when $\|x_t - x_*\| \geq \delta$, we deduce from (66) that

$$\|T_t(x_0, \dots, x_t) - x_*\|^2 \leq (1 + \alpha_t^2 \lambda^2) \|x_t - x_*\|^2 - \alpha_t \lambda \|x_t - x_*\|^2 + \alpha_t^2 B.$$

Otherwise, when $\|x_t - x_*\| \leq \delta$, we have

$$\|T_t(x_0, \dots, x_t) - x_*\|^2 \leq (1 - \alpha_t \lambda)^2 \delta^2 + 2\alpha_t(1 - \alpha_t \lambda) \sqrt{n} \delta (\sigma_t + \mathcal{O}(\epsilon)) + \alpha_t^2 B,$$

where we used $\|x_t - x_*\|_1 \leq \sqrt{n} \|x_t - x_*\| \leq \sqrt{n} \delta$. With the definition

$$a_t = (1 - \alpha_t \lambda)^2 \delta^2 + 2\alpha_t(1 - \alpha_t \lambda) \sqrt{n} \delta (\sigma_t + \mathcal{O}(\epsilon)) + \alpha_t^2 B, \quad (67)$$

we can combine the above two cases as

$$\|T_t(x_0, \dots, x_t) - x_*\|^2 \leq \max\{a_t, (1 + \alpha_t^2 \lambda^2) \|x_t - x_*\|^2 - \alpha_t \lambda \|x_t - x_*\|^2 + \alpha_t^2 B\}.$$

With the additional definitions of

$$b_t = \alpha_t^2 \lambda^2, \quad c_t = \alpha_t \lambda \|x_t - x_*\|^2, \quad h_t = \alpha_t^2 B,$$

we arrive at the key inequality (63).

In order to apply Theorem 5.5, we are left to check the conditions in (64). Using the assumption $\alpha_t \rightarrow 0$, the definition of a_t in (67) implies that $\lim_{t \rightarrow \infty} a_t = \delta^2$. The conditions on $\{b_t\}$ and $\{h_t\}$ are satisfied due to the assumption $\sum_{t=0}^{\infty} \alpha_t^2 \leq \infty$. For $\{c_t\}$, if $\sum_{t=0}^{\infty} c_t < \infty$, then we must have $\|x_t - x_*\|^2 \rightarrow 0$ almost surely because of the assumption $\sum_{t=0}^{\infty} \alpha_t = \infty$, and the conclusion of the theorem holds trivially. Otherwise, $\sum_{t=0}^{\infty} c_t = \infty$ allows all the conditions in (64) to hold, so we can invoke Theorem 5.5 to finish the proof. \square

Following the last remark on Dvoretzky's theorem on page 28, the radius of the neighborhood δ can be refined as follows. Let δ_t be the smallest constant such that $\|x_t - x_*\| \geq \delta_t$ implies

$$2\|x_t - x_*\|_1(c_t + \mathcal{O}(\epsilon)) \leq \lambda\|x_t - x_*\|^2,$$

where σ_t is given by (57). Then we can set $\delta = \limsup_{t \rightarrow \infty} \delta_t$ in (60).

5.4 Bias and variance trade-off

Theorem 5.4 states that the sequence $\{x_t\}$ generated by BCOSW converges almost surely to a neighborhood of x_* , and the radius of the neighborhood is determined by the magnitude of σ_t and ϵ . Specifically, smaller σ_t and ϵ ensure a smaller neighborhood of convergence. According to (57), the magnitude of σ_t depends on both the bias and variance of the estimator v_t . In this section, we examine the delicacy of this bias-variance trade-off and illustrate its effects through several examples.

For convenience, we repeat the definition of σ_t here for quick reference:

$$\sigma_t = \frac{\tau + \mathcal{O}(\tau^2)}{2} + \left(1 + \frac{\tau + \mathcal{O}(\tau^2)}{2}\right) \left\| \frac{-(1/2)\text{Corr}_t(d_t, v_t)}{\sqrt{\text{SNR}_t(d_t)\text{SNR}_t(v_t + \epsilon)}} + \mathcal{O}\left(\frac{1}{\text{SNR}_t(v_t + \epsilon)}\right) \right\|_\infty. \quad (68)$$

Apparently, in order to make σ_t small, it is desirable for the random variable v_t (as an estimator of $\mathbf{E}_t[d_t^2]$) to possess the following properties.

- *Low bias.* This means that Assumption B holds with small τ and ϵ .
- *Low variance*, which naturally leads to *high SNR*. Notice that using a larger ϵ increases $\text{SNR}_t(v_t + \epsilon) = \mathbf{E}_t[v_t + \epsilon]^2 / \text{Var}_t(v_t)$, leading to a smaller σ_t . However, it also increases the $\mathcal{O}(\epsilon)$ term in (58), which affects the radius of neighborhood through (61).

In practice, it is hard to construct estimators with low bias and low variance simultaneously. Below we give several examples to illustrate the trade-off in algorithm design.

1. **Using d_t^2 as the estimator.** The simplest estimator of $\mathbf{E}_t[d_t^2]$ is d_t^2 itself. Setting $v_t = d_t^2$ exhibiting low bias and high variance, specifically,

$$\text{Bias} = |\mathbf{E}_t[v_t] - \mathbf{E}_t[d_t^2]| = 0, \quad \text{Variance} = \text{Var}_t(v_t) = \text{Var}_t(d_t^2).$$

In this case, Assumption B is satisfied with $\tau = 0$ and $\epsilon = 0$. Then we have

$$x_{t+1} = x_t - \alpha_t \frac{d_t}{\sqrt{d_t^2 + \epsilon}} = x_t - \alpha_t \text{sign}(d_t),$$

which corresponds to the sign-gradient method (21) or the sign-momentum method (22), depending on the choice of d_t . Among them, sign-momentum is preferred because $\text{Var}_t(m_t^2)$ is usually much smaller than $\text{Var}_t(g_t^2)$.

2. **Using a constant estimator across coordinates.** Setting $v_t = c\mathbf{1}_n$ for some constant $c > 0$ exhibits high bias and low variance, specifically,

$$\text{Bias} = |\mathbf{E}_t[v_t] - \mathbf{E}_t[d_t^2]| = |c\mathbf{1}_n - \mathbf{E}_t[d_t^2]|, \quad \text{Variance} = \text{Var}_t(v_t) = 0.$$

In this case, we need large τ and ϵ for Assumption B to hold. Correspondingly

$$x_{t+1} = x_t - \alpha_t \frac{d_t}{\sqrt{c\mathbf{1}_n + \epsilon}} = x_t - \alpha'_t d_t,$$

where $\alpha'_t = \alpha_t / \sqrt{c + \epsilon}$ is a scalar stepsize. This is equivalent to the classical SGD with or without momentum, depending on $d_t = m_t$ or $d_t = g_t$ respectively.

3. **Using EMA of d_t^2 as the estimator.** EMA is widely adopted as an online estimator to approximate the mean of a random variable. For example, $v_t = \beta_1 v_{t-1} + (1 - \beta) d_t^2$

is used in BCOS-g (Algorithm 1) and BCOS-m (Algorithm 2) to approximate $\mathbf{E}_t[d_t^2]$, with $d_t = g_t$ and $d_t = m_t$ respectively. The bias can be expressed as

$$\text{Bias} = |\mathbf{E}_t[v_t] - \mathbf{E}_t[d_t^2]| = \left| \mathbf{E}_t \left[\sum_{k=1}^t (1 - \beta) \beta^{t-k} d_k^2 \right] - \mathbf{E}_t[d_t^2] \right|.$$

It is possible to derive a sensible bound on the bias with a smoothness assumption on the loss function, but we do not delve into it here. On the other hand, we have a simple expression for its variance (derivation given in Appendix B.4):

$$\text{Var}_t(v_t) = (1 - \beta)^2 \text{Var}_t(d_t^2),$$

which is much smaller than $\text{Var}_t(d_t^2)$ obtained by simply using d_t^2 as the estimator.

4. **The Adam estimator.** Adam uses stochastic momentum as the search direction, i.e., $d_t = m_t = \beta_1 d_{t-1} + (1 - \beta_1) g_t$. However, it uses the EMA of g_t^2 , rather than the EMA of m_t^2 (as in the previous example), to estimate $\mathbf{E}_t[m_t^2]$. This causes a mismatch from the perspective of BCOS, and it is compensated by using a larger smoothing factor β_2 in the estimator $v_t = \beta_2 v_{t-1} + (1 - \beta_2) g_t^2$. Its bias can be expressed as

$$\text{Bias} = \left| \mathbf{E}_t \left[\sum_{k=1}^t (1 - \beta_2) \beta_2^{t-k} g_k^2 \right] - \mathbf{E}_t \left[\left(\sum_{k=1}^t (1 - \beta_1) \beta_1^{t-k} g_k \right)^2 \right] \right|.$$

Again, deriving a sensible upper bound on the bias can be quite involved and we do not pursue it here. As for the variance, we get (see Appendix B.4)

$$\text{Var}_t(v_t) = (1 - \beta_2)^2 \text{Var}_t(g_t^2).$$

If we choose $\beta_2 = 1 - (1 - \beta_1)^2$, then $\text{Var}_t(v_t) = (1 - \beta_1)^4 \text{Var}_t(g_t^2)$. Therefore, the Adam estimator exhibits a very low variance.

5. **The conditional estimator of BCOS-c.** The BCOS-c method (Algorithm 3) also uses m_t as the search direction. Instead of relying on EMA, it uses a conditional estimator for $\mathbf{E}_t[m_t^2]$, i.e., $v_t = (1 - (1 - \beta)^2) m_{t-1}^2 + (1 - \beta)^2 g_t^2$, where β is the smoothing factor for computing m_t . We have simple expressions for both the bias and the variance:

$$\begin{aligned} \text{Bias}_t(v_t) &= 2\beta(1 - \beta) |m_{t-1} \odot (m_{t-1} - \mathbf{E}_t[g_t])|, \\ \text{Var}_t(v_t) &= (1 - \beta)^4 \text{Var}_t(g_t^2). \end{aligned}$$

Notice that $|m_{t-1} - \mathbf{E}_t[g_t]|$ is the bias of using m_{t-1} to estimate $\mathbf{E}_t[d_t]$, and the bias of v_t can be much smaller than that. Meanwhile, the variance of BCOS-c is the same as Adam when setting β_2 in Adam as $\beta_2 = 1 - (1 - \beta)^2$.

In addition to the bias-variance trade-off illustrated above, the expression of σ_t in (68) also reveals the following tips for algorithm design:

- *High SNR of d_t .* This is consistent with the empirical observation that using the momentum m_t as search direction is often better than using the stochastic gradient g_t , because m_t has much smaller variance, thus higher SNR, than g_t .
- *Positive correlation between d_t and v_t .* The negative sign before $\text{Corr}_t(d_t, v_t)$ implies that a positive correlation can lead to a smaller σ_t . Intuitively, a negative correlation between d_t and v_t may cause large fluctuations of the ratio $d_t/\sqrt{v_t + \epsilon}$.

In summary, our theory captures several essential trade-offs that match intuitions and empirical observations.

6 Conclusion

BCOS is a family of stochastic approximation methods that exploit the flexibility of using different block-coordinate stepsizes. Rather than using sophisticated ideas from optimization, such as preconditioning, it is based on the simple idea of minimizing the distance from the next iterate to an optimal point. While the optimal stepsizes are not computable, we make several simplifications and focus on constructing efficient statistical estimators (for the second moment of the search direction) in determining the stepsizes. In particular, by leveraging a simple conditional estimator, we derive variants of BCOS that achieve competitive performance against AdamW but require less memory and fewer hyperparameters.

Our convergence analysis builds upon several classical results from the stochastic approximation literature. In particular, we extend the classical aiming condition towards a target point to account for coordinate-wise stepsizes and decoupled weight-decay (interpreted as L_2 -regularization). For the conceptual BCOS method, which assumes exact second moment, we establish almost-sure convergence and $\mathcal{O}(1/t)$ rate of convergence. For practical BCOS methods with various second-moment estimators, we establish almost-sure convergence to a neighborhood of the target point, where the radius of the neighborhood is determined by the bias and variance of the second-moment estimator. This framework covers convergence analysis for a broad family of methods, including the sign stochastic gradient/momentum method, RMSProp and Adam(W). In addition, it provides novel insights that can guide the development of new algorithms.

Acknowledgments

We thank Zeyuan Allen-Zhu for helping us with running experiments on GPT2, especially with rotary embedding and distributed data parallelism in PyTorch. We are grateful to Lisa Jin for her codebase that made our lives much easier on experimenting with ResNet and vision Transformers. We also thank Yann Olivier for careful reading of an early version of the draft and providing feedback. Last but not least, we extend our gratitude to Damek Davis, Anil Damle, Adrian Lewis, James Renegar and Katya Scheinberg for their comments and insights that helped us clarify and refine the theoretical underpinnings of the paper.

A PyTorch implementation of BCOS

The following code is also available at <https://github.com/facebookresearch/bcos>.

```
1 import torch
2 from torch.optim import Optimizer
3
4 class BCOS(Optimizer):
5     def __init__(self, params, lr, beta=0.9, eps=1e-6,
6                 weight_decay=0.1, mode='c', decouple_wd=True):
7
8         defaults = dict(lr=lr, beta=beta, eps=eps, wd=weight_decay)
9         super().__init__(params, defaults)
10
11         if mode not in ['g', 'm', 'c']:
12             raise ValueError(f"BCOS mode {mode} not supported")
13         self.mode = mode
14         self.decouple_wd = decouple_wd      # True for BCOSW
15
16     def step(self, closure = None):
17
18         for group in self.param_groups:
19             lr = group["lr"]
20             beta = group["beta"]
21             eps = group["eps"]
22             wd = group["wd"]
23
24             for p in group["params"]:
25                 if not p.requires_grad:
26                     continue
27
28                 state = self.state[p]
29                 g = p.grad
30
31                 # initialize optimizer states for specific modes
32                 if self.mode in ['m', 'c'] and 'm' not in state:
33                     state['m'] = g.detach().clone()
34                 if self.mode in ['g', 'm'] and 'v' not in state:
35                     state['v'] = g.detach().square()
36
37                 # decoupled weight decay or absorb in gradient
38                 if self.decouple_wd:      # p := (1 - lr * wd) * p
39                     p.data.mul_(1 - lr * wd)
40                 else:                      # g := g + wd * p
41                     g.data.add_(p.data, alpha = wd)
42
43                 if self.mode in ['m', 'c']:
44                     m = state['m']
45                     if self.mode == 'c':      # conditional estimator
46                         beta_v = 1 - (1 - beta)**2
47                         g2 = g.detach().square()
48                         v = beta_v * m.square() + (1 - beta_v) * g2
49                     # update momentum
50                     m.mul_(beta).add_(g.detach(), alpha=1 - beta)
51                     d = m
52                 else:
53                     d = g.detach()
54
55                 if self.mode in ['g', 'm']:      # EMA estimator
56                     v = state['v']
57                     v.mul_(beta).add_(d.square(), alpha=1 - beta)
58
59                 # BCOS update: p := p - lr * (d / (sqrt(v) + eps))
60                 p.data.add_(d.div(v.sqrt() + eps), alpha= - lr)
```

B Appendix

B.1 Aiming versus convexity

To illustrate the fundamental differences between the coordinate-wise aiming condition (36) and the standard convexity condition (35), we provide the following two counterexamples, each satisfying one condition while failing the other:

- *Aiming but not convex*: Let $f(x) := \log(x)$ with the optimal solution $x_* = 0$. On the domain of \mathbf{R}_+ , the gradient is $f'(x) = \frac{1}{x}$, and thus $\text{sign}(f'(x)) = 1$ for all $x > 0$. Consequently, for any $x \in \mathbf{R}_+$, we have

$$\langle x - x_*, \text{sign}(\nabla f(x)) \rangle = x \geq 0,$$

satisfying the aiming condition (36). However, $\log(x)$ is a concave function, thus failing the convex inequality (35).

- *Convex but not aiming*: Consider the quadratic function $f : \mathbf{R}^2 \rightarrow \mathbf{R}, f(x) = \frac{1}{2}x^T A x$. Choose the coefficient matrix as

$$A = \begin{pmatrix} 1 \\ -2 \end{pmatrix} \begin{pmatrix} 1 \\ -2 \end{pmatrix}^T = \begin{bmatrix} 1 & -2 \\ -2 & 4 \end{bmatrix} \succeq 0.$$

Since A is positive semidefinite, the function f is convex and attains its minimum at $x_* = \mathbf{0}$. The gradient of f is

$$\nabla f(x) = Ax = \begin{bmatrix} x_1 - 2x_2 \\ -2x_1 + 4x_2 \end{bmatrix}.$$

Evaluating the aiming condition (36) at $x = (1.5, 1)^T$, we get

$$\langle x - x_*, \text{sign}(\nabla f(x)) \rangle = 1.5 \times \text{sign}(-0.5) + 1 \times \text{sign}(1) = 1.5 \times (-1) + 1 \times 1 = -0.5 \leq 0.$$

Thus, the aiming condition (36) does not hold at this point even though f is convex.

B.2 Proof of Lemma 5.5

Proof. The proof leverages the Taylor expansion of $\phi(y) := 1/\sqrt{y}$. Specifically, we have

$$\phi(y + \delta) = \sum_{p=0}^{\infty} \frac{\phi^{(p)}(y)}{p!} \delta^p,$$

where

$$\phi^{(p)} = (-1)^p \left(\frac{1}{2} \cdot \frac{3}{2} \cdots \left(p - \frac{1}{2} \right) \right) y^{-\frac{2p+1}{2}} = (-1)^p \frac{(2p)!}{4^p p!} y^{-\frac{2p+1}{2}}.$$

Taylor expansion (element-wise) at $y = \mathbf{E}_t[d_t^2]$ with $\delta = \mathbf{E}_t[v_t] + \epsilon - \mathbf{E}_t[d_t^2]$ yields the following approximation:

$$\begin{aligned}
\left| \frac{\mathbf{E}_t[d_t]}{\sqrt{\mathbf{E}_t[d_t^2]}} - \frac{\mathbf{E}_t[d_t]}{\sqrt{\mathbf{E}_t[v_t] + \epsilon}} \right| &= |\mathbf{E}_t[d_t](\phi(y) - \phi(y + \delta))| = \left| \mathbf{E}_t[d_t] \left(\sum_{p=1}^{\infty} \frac{\phi^{(p)}(y)}{p!} \delta^p \right) \right| \\
&= \left| \mathbf{E}_t[d_t] \left(\sum_{p=1}^{\infty} (-1)^p \frac{(2p)!}{4^p (p!)^2} \mathbf{E}_t[d_t^2]^{-\frac{2p+1}{2}} (\mathbf{E}_t[v_t] + \epsilon - \mathbf{E}_t[d_t^2])^p \right) \right| \\
&\leq \left| \mathbf{E}_t[d_t] \left(\sum_{p=1}^{\infty} \frac{(2p)!}{4^p (p!)^2} \mathbf{E}_t[d_t^2]^{-\frac{2p+1}{2}} (\tau \mathbf{E}_t[d_t^2] + 2\epsilon)^p \right) \right| \quad (69) \\
&= \left| \mathbf{E}_t[d_t] \left(\sum_{p=1}^{\infty} \frac{(2p)!}{4^p (p!)^2} \mathbf{E}_t[d_t^2]^{-\frac{2p+1}{2}} \tau^p \mathbf{E}_t[d_t^2]^p + \mathcal{O}(\epsilon) \right) \right| \\
&= \left| \frac{\mathbf{E}_t[d_t]}{\sqrt{\mathbf{E}_t[d_t^2]}} \left(\sum_{p=1}^{\infty} \frac{(2p)! \tau^p}{4^p (p!)^2} + \mathcal{O}(\epsilon) \right) \right| \\
&= \frac{\tau + \mathcal{O}(\tau^2)}{2} \left| \frac{\mathbf{E}_t[d_t]}{\sqrt{\mathbf{E}_t[d_t^2]}} \right| + \mathcal{O}(\epsilon)
\end{aligned}$$

where the inequality (69) is a consequence of Assumption B. □

B.3 Proof of Lemma 5.6

We first derive a useful approximation for a general smooth function.

Lemma B.1. *Let $\phi : \mathbf{R}^n \rightarrow \mathbf{R}$ be a smooth (C^∞) function and $X \in \mathbf{R}^n$ a random variable. Then we have*

$$\mathbf{E}[\phi(X)] = \phi(\mathbf{E}[X]) + \frac{1}{2} \langle \nabla^2 \phi(\mathbf{E}[X]), \text{Cov}(X) \rangle + \sum_{|\mathbf{p}|=3}^{\infty} \frac{D^{(\mathbf{p})} \phi(\mathbf{E}[X])}{\mathbf{p}!} \mathbf{E}[(X - \mathbf{E}[X])^{(\mathbf{p})}], \quad (70)$$

where $\langle \cdot, \cdot \rangle$ denotes matrix inner product, i.e., $\langle A, B \rangle = \text{Tr}(A^T B)$. For the multi-variable derivatives, we denote $\mathbf{p} \in \{0, 1, 2, \dots\}^n$, $|\mathbf{p}| = p_1 + \dots + p_n$, $\mathbf{p}! = p_1! \dots p_n!$, and

$$\begin{aligned}
D^{(\mathbf{p})} \phi &= \frac{\partial^{|\mathbf{p}|} \phi}{\partial X^{\mathbf{p}}} = \frac{\partial^{p_1 + \dots + p_n} \phi}{\partial X_1^{p_1} \dots \partial X_n^{p_n}}, \\
(X - \mathbf{E}[X])^{(\mathbf{p})} &= (X_1 - \mathbf{E}[X_1])^{p_1} \dots (X_n - \mathbf{E}[X_n])^{p_n}.
\end{aligned}$$

Proof. Let $\delta := X - \mathbf{E}[X]$ and consider the Taylor expansion of ϕ at $\mathbf{E}[X]$:

$$\phi(X) = \phi(\mathbf{E}[X]) + \nabla \phi(\mathbf{E}[X])^T \delta + \frac{1}{2} \delta^T \nabla^2 \phi(\mathbf{E}[X]) \delta + \sum_{|\mathbf{p}|=3}^{\infty} \frac{D^{(\mathbf{p})} \phi(\mathbf{E}[X])}{\mathbf{p}!} \delta^{(\mathbf{p})}.$$

Taking expectation with respect to X , we have $\mathbf{E}[\delta] = \mathbf{E}[X - \mathbf{E}[X]] = 0$. Therefore,

$$\mathbf{E}[\nabla\phi(\mathbf{E}[X])^T\delta] = \nabla\phi(\mathbf{E}[X])^T\mathbf{E}[\delta] = 0,$$

which, together with the equation $\text{Cov}(X) = \mathbf{E}[\delta\delta^T]$, yields the desired result. \square

Proof of Lemma 5.6. We apply Lemma B.1 with $X := (Y, Z)$ and $\phi(x) = \phi(y, z) := \frac{y}{\sqrt{z}}$. First, the gradient and Hessian of g can be calculated as

$$\nabla\phi(x) = \nabla\phi(y, z) = \begin{pmatrix} \frac{1}{z^{1/2}} \\ y \\ -\frac{y}{2z^{3/2}} \end{pmatrix}, \quad \nabla^2\phi(x) = \nabla^2\phi(y, z) = \begin{bmatrix} 0, & -\frac{1}{2z^{3/2}} \\ -\frac{1}{2z^{3/2}}, & \frac{3y}{4z^{5/2}} \end{bmatrix}.$$

For general p -th partial derivative, we derive the following result for any $q \in \{0, \dots, p\}$:

$$\frac{\partial^p\phi}{\partial y^q \partial z^{p-q}} = \frac{\partial^{p-q}}{\partial z^{p-q}} \left(\frac{\partial^q\phi}{\partial y^q} \right) = \begin{cases} 0 & \text{if } q \geq 2, \\ \frac{\partial^{p-1}}{\partial z^{p-1}} \frac{1}{\sqrt{z}} = (-1)^{p-1} \frac{(2p-2)!}{4^{p-1}(p-1)!} z^{-\frac{2p-1}{2}} & \text{if } q = 1, \\ y \cdot \frac{\partial^p}{\partial z^p} \frac{1}{\sqrt{z}} = (-1)^p \frac{(2p)!}{4^p p!} y z^{-\frac{2p+1}{2}} & \text{if } q = 0. \end{cases}$$

Substitute the Hessian and p -th order partial derivative into (70), we get

$$\begin{aligned} \mathbf{E} \left[\frac{Y}{\sqrt{Z}} \right] &= \frac{\mathbf{E}[Y]}{\sqrt{\mathbf{E}[Z]}} - \mathbf{E} \left[\frac{(Y - \mathbf{E}[Y])(Z - \mathbf{E}[Z])}{2\mathbf{E}[Z]^{3/2}} \right] + \mathbf{E} \left[\frac{3\mathbf{E}[Y](Z - \mathbf{E}[Z])^2}{8\mathbf{E}[Z]^{5/2}} \right] \\ &\quad + \sum_{p=3}^{\infty} \frac{1}{p!} \left(\frac{p(2p-2)!}{4^{p-1}(p-1)!} \mathbf{E} \left[\frac{(Y - \mathbf{E}[Y])(Z - \mathbf{E}[Z])^{p-1}}{\mathbf{E}[Z]^{\frac{2p-1}{2}}} \right] + (-1)^p \frac{(2p)!}{4^p p!} \mathbf{E} \left[\frac{\mathbf{E}[Y](Z - \mathbf{E}[Z])^p}{\mathbf{E}[Z]^{\frac{2p+1}{2}}} \right] \right) \\ &= \frac{\mathbf{E}[Y]}{\sqrt{\mathbf{E}[Z]}} - \frac{\text{Cov}(Y, Z)}{2\mathbf{E}[Z]^{3/2}} + \frac{3\mathbf{E}[Y]\text{Var}(Z)}{8\mathbf{E}[Z]^{5/2}} \\ &\quad + \mathcal{O} \left(\frac{\mathbf{E}[(Y - \mathbf{E}[Y])(Z - \mathbf{E}[Z])^{p-1}]}{\mathbf{E}[Z]^{p-1/2}} \right) + \mathcal{O} \left(\frac{\mathbf{E}[Y]\mathbf{E}[(Z - \mathbf{E}[Z])^p]}{\mathbf{E}[Z]^{p+1/2}} \right) \\ &= \frac{\mathbf{E}[Y]}{\sqrt{\mathbf{E}[Z]}} \left(1 - \frac{\text{Cov}(Y, Z)}{2\mathbf{E}[Y]\mathbf{E}[Z]} + \frac{3\text{Var}(Z)}{8\mathbf{E}[Z]^2} \right. \\ &\quad \left. + \mathcal{O} \left(\frac{\mathbf{E}[(Y - \mathbf{E}[Y])(Z - \mathbf{E}[Z])^{p-1}]}{\mathbf{E}[Y]\mathbf{E}[Z]^{p-1}} \right) + \mathcal{O} \left(\frac{\mathbf{E}[(Z - \mathbf{E}[Z])^p]}{\mathbf{E}[Z]^p} \right) \right), \end{aligned}$$

which is the desired result. \square

B.4 Bias and variance calculation

Here we derive the bias and variance expressions for some estimators listed in Section 5.4.

- **Using EMA of d_t^2 as estimator.** In this case, we have $v_t = \beta_1 v_{t-1} + (1 - \beta) d_t^2$ and

$$\begin{aligned}
 \text{Var}_t(v_t) &= \mathbf{E}_t \left[\left(\sum_{k=1}^t (1 - \beta) \beta^{t-k} d_k^2 - \sum_{k=1}^t (1 - \beta) \beta^{t-k} \mathbf{E}_t[d_k^2] \right)^2 \right] \\
 &= \mathbf{E}_t \left[\left(\sum_{k=1}^{t-1} (1 - \beta) \beta^{t-k} d_k^2 + (1 - \beta) d_t^2 - \sum_{k=1}^{t-1} (1 - \beta) \beta^{t-k} d_k^2 - (1 - \beta) \mathbf{E}_t[d_t^2] \right)^2 \right] \\
 &= (1 - \beta)^2 \mathbf{E}_t \left[(d_t^2 - \mathbf{E}_t[d_t^2])^2 \right] \\
 &= (1 - \beta)^2 \text{Var}_t(d_t^2).
 \end{aligned}$$

- **The Adam estimator.** In this case, we have $v_t = \beta_2 v_{t-1} + (1 - \beta_2) g_t^2$ and

$$\begin{aligned}
 \text{Var}_t(v_t) &= \mathbf{E}_t \left[\left(\sum_{k=1}^t (1 - \beta_2) \beta_2^{t-k} g_k^2 - \sum_{k=1}^t (1 - \beta_2) \beta_2^{t-k} \mathbf{E}_t[g_k^2] \right)^2 \right] \\
 &= \mathbf{E}_t \left[\left(\sum_{k=1}^{t-1} (1 - \beta_2) \beta_2^{t-k} g_k^2 + (1 - \beta_2) g_t^2 - \sum_{k=1}^{t-1} (1 - \beta_2) \beta_2^{t-k} g_k^2 - (1 - \beta_2) \mathbf{E}_t[g_t^2] \right)^2 \right] \\
 &= (1 - \beta_2)^2 \mathbf{E}_t \left[(g_t^2 - \mathbf{E}_t[g_t^2])^2 \right] \\
 &= (1 - \beta_2)^2 \text{Var}_t(g_t^2).
 \end{aligned}$$

- **The conditional estimator of BCOS-c.** In this case, we have $d_t = m_t = \beta m_{t-1} + (1 - \beta) g_t$ and $v_t = (1 - (1 - \beta)^2) m_{t-1}^2 + (1 - \beta)^2 g_t^2$. Therefore,

$$\begin{aligned}
 \text{Bias} &= |\mathbf{E}_t[v_t] - \mathbf{E}_t[d_t^2]| \\
 &= |\mathbf{E}_t[(1 - (1 - \beta)^2) m_{t-1}^2 + (1 - \beta)^2 g_t^2] - \mathbf{E}_t[(\beta m_{t-1} + (1 - \beta) g_t)^2]| \\
 &= |(2\beta - \beta^2) m_{t-1}^2 + (1 - \beta)^2 \mathbf{E}_t[g_t^2] - \beta^2 m_{t-1}^2 - 2\beta(1 - \beta) m_{t-1} \mathbf{E}_t[g_t] - (1 - \beta) \mathbf{E}_t[g_t^2]| \\
 &= |(2\beta - 2\beta^2) m_{t-1}^2 - 2\beta(1 - \beta) m_{t-1} \mathbf{E}_t[g_t]| \\
 &= 2\beta(1 - \beta) |m_{t-1} (m_{t-1} - \mathbf{E}_t[g_t])|,
 \end{aligned}$$

and

$$\begin{aligned}
 \text{Var}_t(v_t) &= \mathbf{E}_t \left[((1 - (1 - \beta)^2) m_{t-1}^2 + (1 - \beta)^2 g_t^2 - (1 - (1 - \beta)^2) m_{t-1}^2 - (1 - \beta)^2 \mathbf{E}_t[g_t^2])^2 \right] \\
 &= (1 - \beta)^4 \mathbf{E}_t \left[(g_t^2 - \mathbf{E}_t[g_t^2])^2 \right] \\
 &= (1 - \beta)^4 \text{Var}_t(g_t^2).
 \end{aligned}$$

References

- [1] L. Balles and P. Hennig. Dissecting Adam: The sign, magnitude and variance of stochastic gradients. In *International Conference on Machine Learning*, pages 404–413. PMLR, 2018.
- [2] J. Bernstein, Y.-X. Wang, K. Azizzadenesheli, and A. Anandkumar. signSGD: Compressed optimisation for non-convex problems. In *International Conference on Machine Learning*, pages 560–569. PMLR, 2018.
- [3] J. R. Blum. Approximation methods which converge with probability one. *The Annals of Mathematical Statistics*, 25(2):382 – 386, 1954.
- [4] J. R. Blum. Multidimensional Stochastic Approximation Methods. *The Annals of Mathematical Statistics*, 25(4):737 – 744, 1954.
- [5] S. Bock, J. Goppold, and M. Weiß. An improvement of the convergence proof of the ADAM-optimizer. *arXiv preprint arXiv:1804.10587*, 2018.
- [6] X. Chen, C. Liang, D. Huang, E. Real, K. Wang, H. Pham, X. Dong, T. Luong, C.-J. Hsieh, Y. Lu, et al. Symbolic discovery of optimization algorithms. *Advances in neural information processing systems*, 36:49205–49233, 2023.
- [7] K. L. Chung. On a stochastic approximation method. *The Annals of Mathematical Statistics*, pages 463–483, 1954.
- [8] A. Defazio, A. Cutkosky, H. Mehta, and K. Mishchenko. Optimal linear decay learning rate schedules and further refinements, 2024.
- [9] A. Défossez, L. Bottou, F. Bach, and N. Usunier. A simple convergence proof of Adam and Adagrad. *arXiv preprint arXiv:2003.02395*, 2020.
- [10] B. Delyon and A. Juditsky. Accelerated stochastic approximation. *SIAM Journal on Optimization*, 3(4):868–881, 1993.
- [11] J. Deng, W. Dong, R. Socher, L.-J. Li, K. Li, and L. Fei-Fei. Imagenet: A large-scale hierarchical image database. In *2009 IEEE Conference on Computer Vision and Pattern Recognition*, pages 248–255, 2009.
- [12] C. Derman and J. Sacks. On Dvoretzky’s Stochastic Approximation Theorem. *The Annals of Mathematical Statistics*, 30(2):601 – 606, 1959.
- [13] E. Dinan, S. Yaida, and S. Zhang. Effective theory of transformers at initialization. *arXiv preprint arXiv:2304.02034*, 2023.
- [14] J. Duchi, E. Hazan, and Y. Singer. Adaptive subgradient methods for online learning and stochastic optimization. *Journal of Machine Learning Research*, 12(Jul):2121–2159, 2011.

- [15] A. Dvoretzky. On stochastic approximation. In *Proceedings of the Third Berkeley Symposium on Mathematical Statistics and Probability*, volume 1, pages 39–55. University of California Press, 1956.
- [16] A. Gokaslan and V. Cohen. Openwebtext corpus. <http://Skylion007.github.io/OpenWebTextCorpus>, 2019.
- [17] D. M. Gomes, Y. Zhang, E. Belilovsky, G. Wolf, and M. S. Hosseini. AdaFisher: Adaptive second order optimization via Fisher information. *arXiv preprint arXiv:2405.16397*, 2024.
- [18] A. M. Gupal and L. T. Bazhenov. A stochastic analog of the conjugate gradient method. *Cybernetics*, 8(1):138–140, 1972.
- [19] T. Hastie, R. Tibshirani, and J. Friedman. *The elements of statistical learning: data mining, inference and prediction*. Springer, 2nd edition, 2009.
- [20] K. He, X. Zhang, S. Ren, and J. Sun. Delving deep into rectifiers: Surpassing human-level performance on imagenet classification. In *Proceedings of the IEEE international conference on computer vision*, pages 1026–1034, 2015.
- [21] K. He, X. Zhang, S. Ren, and J. Sun. Deep residual learning for image recognition. In *2016 IEEE Conference on Computer Vision and Pattern Recognition (CVPR)*, pages 770–778, 2016.
- [22] D. Hwang. FAdam: Adam is a natural gradient optimizer using diagonal empirical Fisher information. *arXiv preprint arXiv:2405.12807*, 2024.
- [23] R. A. Jacobs. Increased rates of convergence through learning rate adaption. *Neural Networks*, 1:295–307, 1988.
- [24] W. Jiang, S. Yang, W. Yang, and L. Zhang. Efficient sign-based optimization: Accelerating convergence via variance reduction. In *The Thirty-eighth Annual Conference on Neural Information Processing Systems*, 2024.
- [25] K. Jordan, Y. Jin, V. Boza, J. You, F. Cesista, L. Newhouse, and J. Bernstein. Muon: An optimizer for hidden layers in neural networks, 2024. URL: <https://kellerjordan.github.io/posts/muon/>.
- [26] H. Kesten. Accelerated stochastic approximation. *Annals of Mathematical Statistics*, 29(1):41–59, 1958.
- [27] D. P. Kingma and J. Ba. Adam: A method for stochastic optimization. In *Proceedings of International Conference on Learning Representations (ICLR)*, 2015. arXiv:1412.6980.
- [28] A. Krizhevsky and G. Hinton. Learning multiple layers of features from tiny images. Technical Report 0, University of Toronto, Toronto, Ontario, 2009.

- [29] F. Kunstner, A. Milligan, R. Yadav, M. Schmidt, and A. Bietti. Heavy-tailed class imbalance and why Adam outperforms gradient descent on language models. *Advances in Neural Information Processing Systems*, 37:30106–30148, 2024.
- [30] H. J. Kushner and G. G. Yin. *Stochastic Approximation and Recursive Algorithms and Applications*. Springer, 2nd edition, 2003.
- [31] W. Lin, F. Dangel, R. Eschenhagen, J. Bae, R. E. Turner, and A. Makhzani. Can we remove the square-root in adaptive gradient methods? a second-order perspective. *arXiv preprint arXiv:2402.03496*, 2024.
- [32] I. Loshchilov and F. Hutter. Sgdr: Stochastic gradient descent with warm restarts. *arXiv preprint arXiv:1608.03983*, 2016.
- [33] I. Loshchilov and F. Hutter. Decoupled weight decay regularization. In *International Conference on Learning Representations (ICLR)*, 2019.
- [34] A. R. Mahmood, R. S. Sutton, T. Degris, and P. M. Pilarski. Tuning-free step-size adaption. In *Proceedings of the IEEE International Conference on Acoustics, Speech and Signal Processing (ICASSP)*, pages 2121–2124, 2012.
- [35] F. Mirzakhmedov and S. P. Uryasev. Adaptive step adjustment for a stochastic optimization algorithm. *Zh. Vychisl. Mat. Mat. Fiz.*, 23(6):1314–1325, 1983. [U.S.S.R. Comput. Math. Math. Phys. 23:6, 1983].
- [36] Y. Nesterov. *Introductory Lecture on Convex Optimization: A Basic Course*. Kluwer Academic Publishers, 2004.
- [37] T. Pethick, W. Xie, K. Antonakopoulos, Z. Zhu, A. Silveti-Falls, and V. Cevher. Training deep learning models with norm-constrained LMOs. In *Proceedings of the 21st International Conference on Machine Learning (ICML)*, 2025. arXiv:2502.07529.
- [38] B. T. Polyak. Comparison of the rates of convergence of one-step and multi-step optimization algorithms in the presence of noise. *Engineering Cybernetics*, 15:6–10, 1977.
- [39] B. T. Polyak and Y. Z. Tsypkin. Pseudogradient adaptation and training algorithms. *Automation and Remote Control*, a translation of *Avtomatika i Telemekhanika*, 34(3):377–397, 1973.
- [40] A. Radford, J. Wu, R. Child, D. Luan, D. Amodei, and I. Sutskever. Language models are unsupervised multitask learners. OpenAI Tech Report, 2019.
- [41] S. J. Reddi, S. Kale, and S. Kumar. On the convergence of Adam and beyond. *arXiv preprint arXiv:1904.09237*, 2019.
- [42] H. Robbins and S. Monro. A stochastic approximation method. *The Annals of Mathematical Statistics*, 22(3):400–407, 1951.

- [43] H. Robbins and D. Siegmund. A convergence theorem for non negative almost supermartingales and some applications. In J. S. Rustagi, editor, *Optimizing Methods in Statistics*, pages 233–257. Academic Press, 1971.
- [44] D. A. Roberts, S. Yaida, and B. Hanin. *The Principles of Deep Learning Theory: An Effective Theory Approach to Understanding Neural Networks*. Cambridge University Press, 2022.
- [45] A. Ruszczyński and W. Syski. Stochastic approximation method with gradient averaging for unconstrained problems. *IEEE Transactions on Automatic Control*, 28(12):1097–1105, 1983.
- [46] A. Ruszczyński and W. Syski. Stochastic approximation algorithm with gradient averaging and on-line stepsize rules. In J. Gertler and L. Keviczky, editors, *Proceedings of 9th IFAC World Congress*, pages 1023–1027, Budapest, Hungary, 1984.
- [47] M. Safaryan and P. Richtarik. Stochastic sign descent methods: New algorithms and better theory. In M. Meila and T. Zhang, editors, *Proceedings of the 38th International Conference on Machine Learning*, volume 139 of *Proceedings of Machine Learning Research*, pages 9224–9234. PMLR, 18–24 Jul 2021.
- [48] D. J. Sakrison. Stochastic approximation: A recursive method for solving regression problems. In A. Balakrishnan, editor, *Advances in Communication Systems*, volume 2, pages 51–106. Elsevier, 1966.
- [49] N. N. Schraudolph. Local gain adaptation in stochastic gradient descent. In *Proceedings of Ninth International Conference on Artificial Neural Networks (ICANN)*, pages 569–574, 1999.
- [50] R. S. Sutton. Adapting bias by gradient descent: An incremental version of Delta-Bar-Delta. In *Proceedings of the Tenth National Conference on Artificial Intelligence (AAAI’92)*, pages 171–176. The MIT Press, 1992.
- [51] T. Tieleman and G. Hinton. Lecture 6.5-rmsprop: Divide the gradient by a running average of its recent magnitude. *COURSERA: Neural networks for machine learning*, 4(2):26–31, 2012.
- [52] H. Touvron, M. Cord, M. Douze, F. Massa, A. Sablayrolles, and H. Jegou. Training data-efficient image transformers and distillation through attention. In M. Meila and T. Zhang, editors, *Proceedings of the 38th International Conference on Machine Learning*, volume 139 of *Proceedings of Machine Learning Research*, pages 10347–10357. PMLR, 18–24 Jul 2021.
- [53] J. H. Venter. On Dvoretzky Stochastic Approximation Theorems. *The Annals of Mathematical Statistics*, 37(6):1534 – 1544, 1966.

- [54] M. T. Wasan. *Stochastic Approximation*. Cambridge University Press, 1969.
- [55] J. Wolfowitz. On the stochastic approximation method of Robbins and Monro. *The Annals of Mathematical Statistics*, 23(3):457–461, 1952.
- [56] Z. Yao, A. Gholami, S. Shen, M. Mustafa, K. Keutzer, and M. Mahoney. Adahessian: An adaptive second order optimizer for machine learning. In *proceedings of the AAAI conference on artificial intelligence*, volume 35, pages 10665–10673, 2021.
- [57] Y. Zhang, C. Chen, Z. Li, T. Ding, C. Wu, D. P. Kingma, Y. Ye, Z.-Q. Luo, and R. Sun. Adam-mini: Use fewer learning rates to gain more. *arXiv preprint arXiv:2406.16793*, 2024.
- [58] Y. Zhang, C. Chen, N. Shi, R. Sun, and Z.-Q. Luo. Adam can converge without any modification on update rules. In S. Koyejo, S. Mohamed, A. Agarwal, D. Belgrave, K. Cho, and A. Oh, editors, *Advances in Neural Information Processing Systems*, volume 35, pages 28386–28399. Curran Associates, Inc., 2022.
- [59] F. Zou, L. Shen, Z. Jie, W. Zhang, and W. Liu. A sufficient condition for convergences of Adam and RMSProp. In *Proceedings of the IEEE/CVF Conference on computer vision and pattern recognition*, pages 11127–11135, 2019.